CHEMISTRY
A EUROPEAN JOURNAL

New Chiral Auxiliaries for Dynamic Kinetic Resolution: From Theory to Experiment

A. Gil Santos,*[a] Jorge Pereira,[a, b] Carlos A. M. Afonso,[c] and Gernot Frenking[d]

Abstract: New efficient chiral auxiliaries for dynamic kinetic resolution (DKR) of bromides into amines are proposed, based on a theoretical rationalisation of known literature results. One example was synthesized and tested, affording diastereoselectivities up to 100%. Several results of DKR reactions are known, based on oxazolidinone or imidazolidinone units as chiral auxiliaries. Nevertheless, their behaviour was not fully understood until a recent paper that we published. We now used our proposed mechanism to rationalize the behaviour of other similar chiral auxiliaries and to propose small structure changes in imidazolidinone rings which could largely improve their performance. We could show that the good performance of these molecules as chiral auxiliaries for DKR reactions where bromine is the leaving group and a primary or secondary amine is the nucleophile is due, in a first step, to the formation of a hydrogen bond between the amine and the ring carbonyl oxygen and, in a second step, to the strong electrostatic interaction between the leaving bromide and the carbonyl oxygen in the C-3 substituent. Considering the behaviour of this substituent which rotates to minimize the electrostatic repulsion with the bromide when reaching the transition state, we proposed the introduction of a second substituent in the C-4 position of the imidazolidinone ring, which prevents such rotation, thus increasing the energy difference between the transition states of the two diastereoisomers. With such an auxiliary we were able to increase the best *de* known in literature (88%), when benzylamine is used as nucleophile, to 99, or even 100%, when iodide replaces the bromide in the substrate.

Keywords: ab initio calculations · asymmetric synthesis · chiral auxiliaries · kinetic resolution · transition states

Introduction

Chiral auxiliaries are at present time widely used as chemical blocks able to induce chirality in several known synthetic strategies.[1–9] After the synthesis, these units are removed and, at least in principle, they can be reused ad infinitum. Two interesting families of compounds, which are used for more then twenty years, are oxazolidinones **1** and imidazolidinones **2**. As, for our purpose, both families show identical behaviour, we will treat them as a unique family.[10–18]

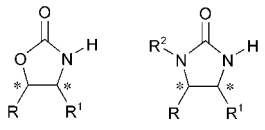

1 **2**

The excellent behaviour of this family of compounds as chiral auxiliaries is mainly due to their low flexibility. In fact, these auxiliaries are very rigid structures, formed by a five-membered ring which is usually connected to the substrate by an amide bond (Scheme 1). The system can rotate through this bond but, since the calculated energy difference

[a] Prof. A. G. Santos, Dr. J. Pereira
Requimte, CQFB, Chemistry Department
Faculdade de Ciências e Tecnologia
Universidade Nova de Lisboa
2829-516 Caparica (Portugal)
Fax: (+351) 212-948-550
E-mail: ags@dq.fct.unl.pt

[b] Dr. J. Pereira
Escola Superior de Tecnologia de Setúbal
Instituto Politécnico de Setúbal
2910-761 Setúbal (Portugal)

[c] Prof. C. A. M. Afonso
CQFM, Department of Chemical Engineering
Instituto Superior Técnico
1049-001 Lisboa (Portugal)

[d] Prof. G. Frenking
Fachbereich Chemie, Philipps-Universität Marburg
Hans-Meerwein-Strasse, 35032 Marburg (Germany)

DOI: 10.1002/chem.200400512

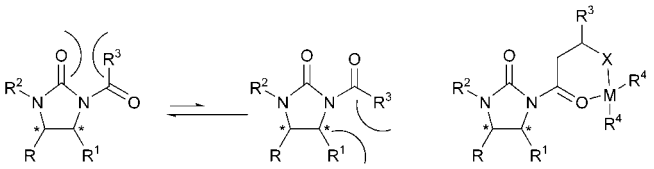

Scheme 1. Possible interactions in imidazolidinone derivatives.

is very high (>30 kJ mol^{-1}[19])—because of a large change in the dipole moment—the equilibrium is strongly shifted to the anti-coplanar side. The side chain can have destabilizing steric interactions with the ring carbonyl group and the ring substituent, which also reduces the number of possible conformers.[14,16–18] If the side chain contains functional groups with the possibility of forming chelates with Lewis acids and the carbonyl groups, then we get another way to control the system rigidity.[12,16,18] Since the most important condition to achieve a high degree of stereocontrol in asymmetric synthesis is the rigidity of the transition state or, in another words, the low number of probable conformers, the properties of this system make it a very interesting chiral auxiliary.

The first published reports on the use of oxazolidinones or imidazolidinones describe their use as chiral auxiliaries in ionic reactions. The basis for an explanation of the reaction mechanism is the work of Evans et al. about twenty years ago.[11–14,17,18] After this, many results were published, both on ionic[16,20–23] and radical reactions[24–29] (Scheme 2) and even on dynamic kinetic resolutions (DKR) (Scheme 3).[30–40]

In spite of the diastereoisomeric excess (*de*) in different types of reactions being usually higher than 80 up to 95%, an unexpected stereochemistry is obtained considering the steric hindrance due to the ring substituent (Scheme 2). To explain this observation, Evans proposed a mechanism (Scheme 2) where the stereochemistry can be understood assuming that the reacting conformer is the one where the two carbonyl groups are coplanar due to their complexation with the Lewis acid.[18] After Evans, it was assumed that this was the explanation for all reactions where this stereochemistry was obtained (almost all cases). In the cases where the "expected" stereochemistry was reached, the explanation was always that no complexation took place, with the attack from the less hindered face yielding the other possible epimer (Scheme 2).

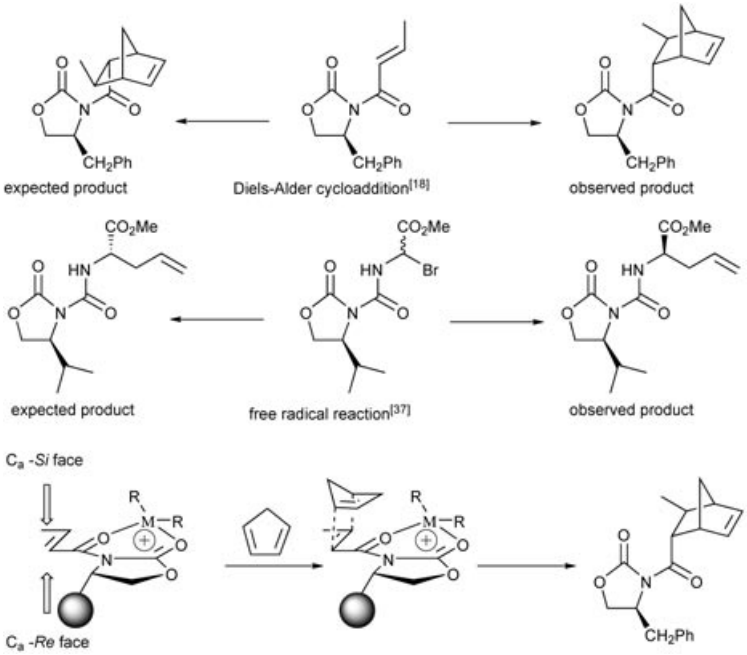

Scheme 2. Use of oxazolidinones as chiral auxiliaries in cycloadditions and in free radical reactions. Bottom: Mechanism proposed by Evans et al.[18] to explain their experimental results on cycloadditions.

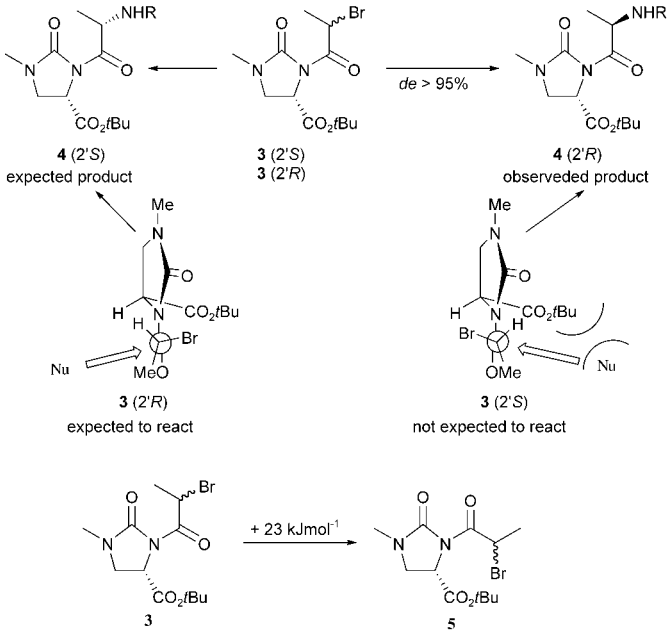

Scheme 3. Observations made by Nunami et al.[34–36] on DKR reactions. Expected versus experimental observed products.

About ten years ago Nunami et al.[34,35] found that compound **3**, when treated with secondary or primary amines under DKR conditions, afforded the epimer **4** (2′*R*) in more than 95% *de* (depending on the amine used) (Scheme 3) which was in disagreement with their initial hypothesis that the amine would easily attack the 2′*R*-bromine isomer **3** from the less hindered face. Notably this stereoselectivity is exactly the same as that obtained by Evans and following workers in the field. Nevertheless, contrary to Evans, Nunami could not explain his results with some kind of chela-

tion where the carbonyl groups would be coplanar. He also calculated[36] the energy difference between the two conformers (molecular mechanics) and found that the value was too large (around 23 kJ mol^{-1}) to easily favour the coplanar orientation **5**.

A mechanism was proposed where a hydrogen-bonding interaction between the amine and the carbonyl on the ring substituent would direct the attack from the most hindered face (Figure 1). In accordance with this, nucleophiles which are not capable of hydrogen bonding yielded the "expected" stereochemistry.[37–39]

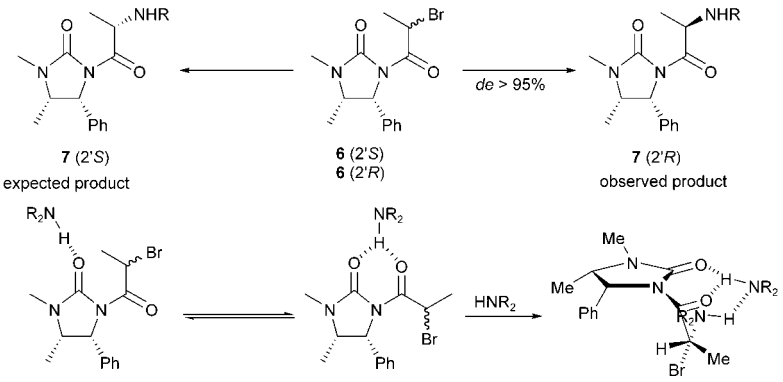

Scheme 4. Experimental observations made by Caddick et al.[32] and their proposed mechanism.

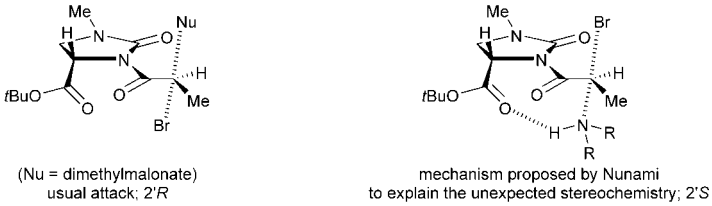

Figure 1. Reaction mechanism proposed by Nunami et al.[37–39] to explain their experimental observations.

A few years ago, Caddick et al.[31,32] found that the treatment of compound **6** with primary or secondary amines under DKR conditions similar to those used by Nunami yielded epimer **7** (2′*R*) (Scheme 4), which is again the unexpected isomer. Since there is no possibility for hydrogen bonding as suggested by Nunami, Caddick proposed a different mechanism where a hydrogen bond between the amine and the two carbonyl groups would shift the equilibrium from the anti- to the coplanar conformation (Scheme 4). A second amine would make another hydrogen bond, directing the attack through the less hindered face.[32]

Our involvement in Caddick's work brought us to another proposal[19,41] where an interaction between the leaving group (bromide) and the aromatic ring in the auxiliary moiety (Figure 2) can explain all the experimental observations; this would avoid the need for the formation of a rather unlikely complex as that in Scheme 4.

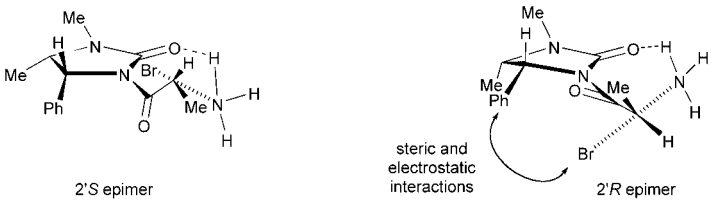

Figure 2. Reaction mechanism proposed by us[19] as an alternative to Caddick's mechanism, based on theoretical results obtained at HF/3-21G*.

In this paper we wish to improve the results we published before[19] introducing new data to explain Nanami's observations. We propose subtle but rationalized structural modifications to known chiral auxiliaries, which can significantly improve their performance. The synthesis of some examples will be discussed as well as their experimental performance as chiral auxiliaries in selected DKR reactions.

Results and Discussion

Theoretical studies: In our previous paper[19] we proposed a reaction mechanism for Caddick's system[32,41] based on calculated transition states at HF/3-21G*. The results were enthalpic values (ΔH), calculated by subtracting the enthalpy of the amine complex from that of the transition state (Figure 3). In this paper we use free energy values (ΔG), which were calculated at higher levels of theory. The activation energy ($\Delta G^{\neq}$) is calculated by subtracting the free energy of the uncomplexed amine and substrate from that of the transition state (Figure 3). This approach appears to us more correct, since the amine complex must have a higher energy than that of the free amine and free substrate, as shown from the experimental results (no complex was observed by NMR experiments) and also from the theoretical results when the entropy is considered.

Our previous paper[19] employed a rather small basis set due to limited computational resources[42] which yielded energies that could not be considered as very accurate. The present results have been obtained at a higher level of theory[1] which should be more reliable.[43]

Structure **8** (Table 1) was used by Nunami[36] in order to test his proposed model. If the mechanism shown in Figure 1 is correct, the reduction of the carboxyl group to ether would avoid hydrogen-bond formation yielding consequent changes in the stereochemistry. Only a strong reduc-

[1] Full geometry optimizations have been performed employing HF or DFT theories, with no symmetry restrictions, by using Gaussian 98[43] and default optimization criteria. MP2 energies were obtained as single-point calculations (MP2 (full)) over HF-optimized structures. Electronic surfaces were calculated with Spartan,[42] by using a value of 0.002 e$^-$ au^{-3} at HF 6-31G**.

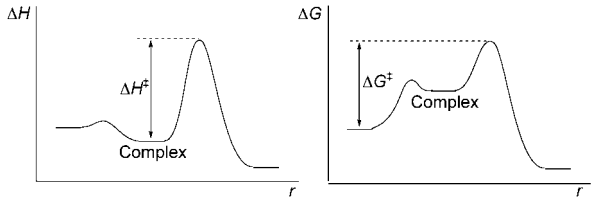

Figure 3. Transition state activation energies. Left: enthalpy, measured as the energy difference between the complex and the TS structure and, right: Gibbs energy measured as the energy difference between the reagents and the TS structures.

tion in the *de* value was observed, but not inversion of configuration; this indicates that the mechanism must be different from that one shown in Figure 1. As it can be seen in Table 1, the values obtained at HF/3-21G* are oscillating, particularly for structure **3**. Nevertheless, the basis set performs acceptably for structure **6** and therefore, the previous results appear to be acceptable. The values obtained at MP2/6-31G**//HF/3-21G* are more consistent but the value for compound **8** still indicates the opposite stereochemistry.

Table 1. Transition state Gibbs energy differences (epimer 2′*R*−epimer 2′*S*) for compounds **6**, **3** and **8** with comparison of theoretical and experimental diastereomeric excesses.[a–c]

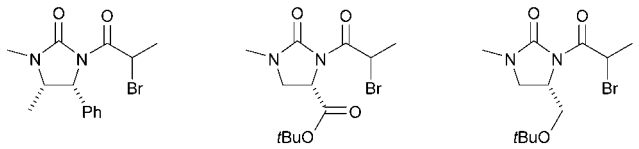

6 **3** **8**

Structure	Method	$\Delta G^{\ddagger}_{2'R}-\Delta G^{\ddagger}_{2'S}$ [kJ mol^{-1}]	*de* [%] calcd	exptl
6	HF/3-21G*	13.4	99.1	<90
	MP2/6-31G**//HF/3-21G*	7.0	88.8	
	MP2/6-31G**//HF/6-31G**[a]	7.3	90.0	
	PW91/6-31G**[b]	7.3	90.0	
3	HF/3-21G*	38.3	>99.9	<96
	MP2/6-31G**//HF/3-21G*	13.3	99.1	
	MP2/6-31G**//HF/6-31G**[a]	12.4	98.7	
	PW91/6-31G**[b]	12.3	98.6	
8	HF/3-21G*	0.9	17.9	≈35
	MP2/6-31G**//HF/3-21G**	−1.2	−23.7	
	MP2/6-31G**//HF/6-31G**[a]	2.4	44.2	
	PW91/6-31G**[b]	2.0	38.9	

[a] Scaling factor $a=1.58$. [b] Scaling factor $b=1.78$. [c] The values were obtained after division by the scaling factor. The scaling factors were calculated in order to obtain energy differences for compound **6** of about 7.3 kJ mol (90% *de*).

With larger basis sets at MP2/6-31G**//HF/6-31G** or PW91/6-31G**[44] the results are in good agreement with the experimental data after application of a normalization factor. Since both Nunami's and Caddick's results show a wide range of *de* values, we decided to use a value of 90% *de* for Caddick's auxiliary, which is near the upper side of his range of values. By using the same factor for Nunami's auxiliary, we can see that the theoretical values are higher, in accordance with the experimental results. Also, both MP2//HF or DFT make a good prediction of the expected *de* for compound **8**.

The values in Table 1 were obtained by using ammonia as the attacking group. Nevertheless, since the best experimental data was reached with several different amines, we decided to perform a few tests to dismiss any transition state energy dependence on the attacking group. We used three different amines and Nunami's auxiliary, as depicted in Table 2. No strong dependence on the attacking group can

Table 2. Effect of different amines on the TS as Gibbs energy differences.

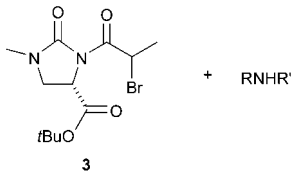

3

Method	$\Delta G^{\ddagger}_{2'R}-\Delta G^{\ddagger}_{2'S}$ [kJmol^{-1}] R=H R′=H	R=Me R′=H	R=Me R′=Me	R=*t*Bu R′=H
HF/3-21G*	38.3	33.2	36.2	34.0
MP2/6-31G**//HF/3-21G*	13.3	10.8	10.9	11.2
MP2/6-31G**//HF/6-31G**[a]	12.4	12.4	12.2	11.6
PW91/6-31G**[b]	12.3	11.8	12.9	12.8

[a] Scaling factor $a=1.58$. [b] Scaling factor $b=1.78$.

be observed. The results are similar to those obtained with ammonia and show that, in the transition state, there are no strong interactions between the attacking group and the auxiliary when small amines are used. The important differences observed experimentally, when different amines are used as nucleophiles are probably caused by a strong dependence on hydrogen-bond formation when solvents are used.

While the energy values of the transition states for each epimer are very sensible to the basis set used, the geometries do not vary much. Nevertheless, the transition state geometries for different 2′*R* epimers show larger differences, which indicates also larger differences in the molecular interactions they are experiencing. Contrarily, the TS structures of the 2′*S* epimers are more similar, since both the leaving and attacking groups do not have strong interactions with the rest of the molecule.

Analysing first the 2′*S* epimers we can say that the energy minimum structures at HF/3-21G* exhibit strong hydrogen bonds which have shorter bond lengths compared with HF/6-31G**. In the case of compound **3** (TS, epimer 2′*S*) two hydrogen bonds are formed as depicted in Figure 4. One of the rotamers of compound **8** (TS, epimer 2′*S*) even has a second hydrogen bond between the ether oxygen and the amine (**8b**) but with a higher transition state energy (about 11 kJ mol^{-1}) relative to conformer **8a** (ts).

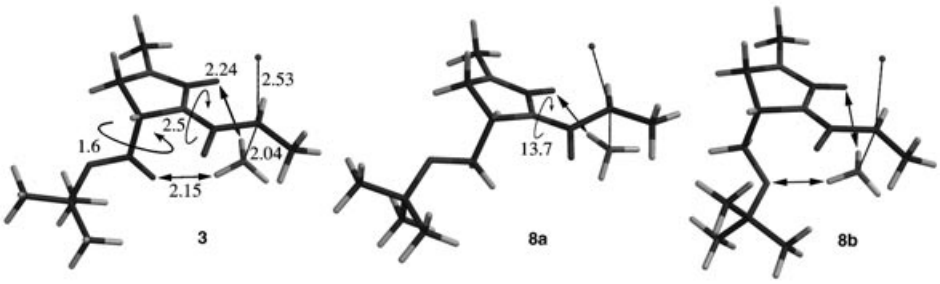

Figure 4. Transition state structures for compounds **3** (2′*S*) and **8** (2′*S*) calculated at HF/3-21G*. Distances in Å and angles in degrees.

When minimising the structures using HF/6-31G** no second hydrogen bond was observed for any one of the compounds. At the PW91/6-31G** level the C–Br partial bond and the hydrogen bond are much shorter than the equivalent ones obtained at the HF theory, as observed for compound **3** (Figure 5). A similar result was obtained at both levels of theory for all transition state structures.

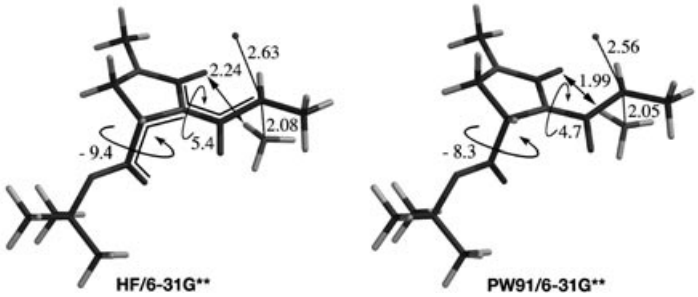

Figure 5. Transition state structures for compound **3** (2′*S*), calculated at HF/6-31G** (left) and (right) at PW91/6-31G**. Distances in Å and angles in degrees (the negative angles mean that, contrary to Figure 4, the carbonyl bond points inside the ring).

Thus, we can say that structures optimized at HF/3-21G* are quite accurate for starting materials, but are not so good for transition states, with strong differences in the angles of the amide bond and also in the lengths of some bonds.

If we now analyse the behaviour of 2′*R* epimers, very interesting effects can be found. Since in these epimers there is a strong contact (stereo and/or electrostatic) between the leaving group and the substituent's auxiliary, strong changes can also be observed in order to lower the TS energy. In Nunami's auxiliary (**3** (2′*R*)) the ring substituent rotates, taking the carbonyl group away from the halogen leaving group (Figure 6). In the case of Caddick's auxiliary (**6** (2′*R*)), a similar rotation is not observed. Instead, a second effect occurs, where the entire five-membered ring is distorted. This brings the aromatic ring and the bromine atom away from each other. Interestingly the rotation of the aromatic ring would diminish the steric interactions between the aromatic ring and the bromine atom. But, since the centre of the ring has a negative charge and the electrostatic repulsive interaction with the bromine atom would thus increase the energy of the system, the final adopted conformation of the molecule brings the positive charge of the aromatic ring close to the bromine atom through the formation of a hydrogen bond (Figure 7).

In Nunami's auxiliary (**3** (2′*R*)) the five-membered ring does not change much between the initial structure and the

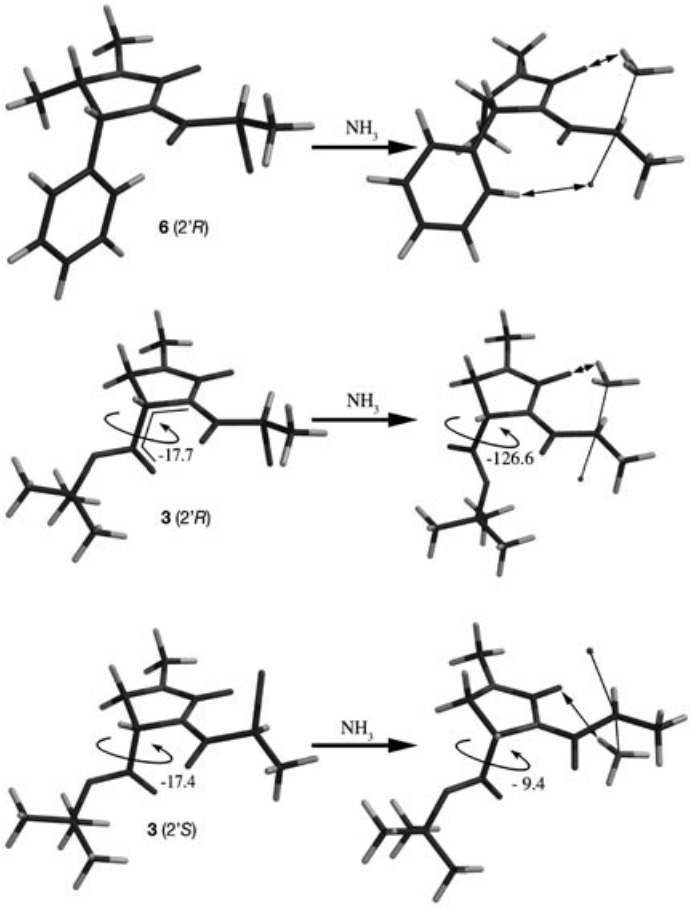

Figure 6. Transition state structures of compounds **3** (2′*R*), (2′*S*) and **6** (2′*R*) at HF/6-31G**. Angles in degrees (the negative angles have the same meaning as in Figure 5.

transition state. The energy decrease is reached by the rotation of the group (Figure 6). This rotation brings the *tert*-butyl group close to the leaving group but, since the electrostatic interactions between the carboxyl oxygen and the bromine atom are very strong (Figure 7), it compensates for the increase in steric interaction. Looking at structure **3** (2′*R*) (Figure 7), one can see that the large rotation happens not only due to the repulsion between the leaving bromide and the carboxyl oxygen, but also due to the attraction (formation of hydrogen bond) between the leaving bromide and

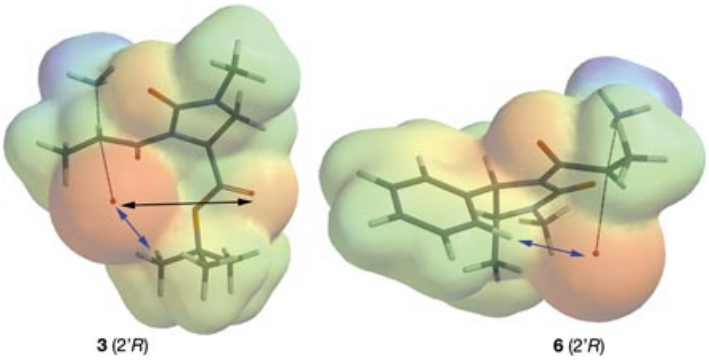

Figure 7. Electronic isodensity surfaces ($0.002\,e^{-}au^{-3}$, HF/6-31G**) mapped with the electrostatic potential, for TS structures of compounds **3** (2′*R*) and **6** (2′*R*), showing the electrostatic interactions (repulsive interactions: black arrows; attractive interactions: blue arrows) between the leaving bromide and the auxiliary substituent. Red zones indicate negative potential and blue zones indicate positive potential.

the hydrogen atoms in the *tert*-butyl group. Without this interaction the rotation would not take place to such a large extent. When we compare the dihedral angles for both 2′ epimers of compound **3** (Figure 6) we can see that for epimer *R* the side chain angle increases by more than 100°, while for epimer *S* there is a decrease by about 8°. The large difference shows how important the electrostatic interactions become in such systems (Figure 7), which explains the excellent behaviour of Nunami's auxiliary in this type of DKR reactions.

A strategy to increase the energy difference between the epimers 2′*S* and 2′*R* would be to change the geometry of the latter with the goal to make the rotation of the substituent more difficult, because the epimer 2′*S* has already the optimal form. Many structure alterations can be proposed to reach this effect. If calculations would yield suitably modified compounds, then the choice between them will be just a matter of experimental viability. One of them is compound **9**, which is a simple methyl derivative of Nunami's auxiliary. Another example possesses a different structure with two fused rings **10**, but the theoretically predicted effect should be similar (Table 3). The structures and the transition states

Table 3. Transition state Gibbs energy differences (epimer 2′*R*−epimer 2′*S*) for compounds **9** and **10** and theoretical diastereomeric excesses.

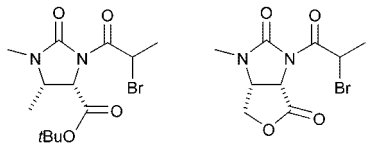

Method	$\Delta G^{+}_{2'R}-G^{+}_{2'S}$ [kJ mol^{-1}] and *de* [%] **9** (ts)		**10** (ts)	
HF/3-21G*	38.3	>99.9	22.4	>99.9
MP2/6-31G**//HF/3-21G*	19.5	99.9	6.2	84.8
MP2/6-31G**//HF/6-31G**[a]	18.3	99.9	17.7	99.8
PW91/6-31G**[b]	15.5	99.6	15.6	99.6

[a] Scaling factor $a=1.58$. [b] Scaling factor $b=1.78$.

of the reactions with ammonia were optimized with the same methods used for the known auxiliaries. The TS energies were scaled using the same factors we used before. The results are summarised in Table 3 and the 3D structures are shown in Figures 8 and 9.

Comparing the energy differences, we can see again a quite good agreement between the results obtained at MP2/6-31G**//HF/6-31G** and those obtained with DFT at PW91/6-31G**.

If we now compare the TS 3D structures of compounds **3** and **9** (2′*R* epimers) (Figure 8), we can see that the rotation of the ring substituent in structure **9** is only −70.8°, while in structure **3** it is −126.6°. Further differences are also observed in the amide bond rotation (smaller value in structure **9**) and in the length of the hydrogen bond (shorter in structure **9**). Comparing the energies in Table 3 (structure **3**) with those in Table 1, we can notice an energy increase between 3 and 6 kJ mol^{-1} for structure **9** and between 3 and 5.5 kJ mol^{-1} for structure **10** (PW91/6-31G** and MP2/6-31G**//HF/6-31G**, respectively). This difference is enough to increase the expected *de* to near 100%.

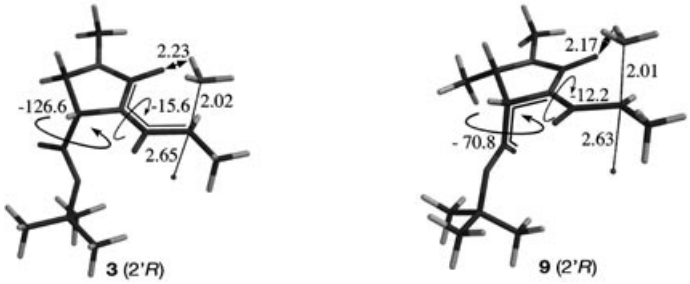

Figure 8. Transition state 3D models for structures **3** and **9**, epimers 2′*R*, at HF/6-31G**. Distances in Å and angles in degrees (the negative angles shall be compared with those in Figures 4 and 5).

It is interesting to analyse in more detail the TS 3D structures of compounds **6** and **10**, epimers 2′*R* (Figure 9). In both cases it can be seen that the molecule finds a conformation where the leaving bromine atom makes a hydrogen bond with one hydrogen of the aromatic ring (compound **6**) or with one hydrogen of the second five-membered ring (compound **10**). The formation of this type of hydrogen bond is reasonable. Any factor which makes the formation

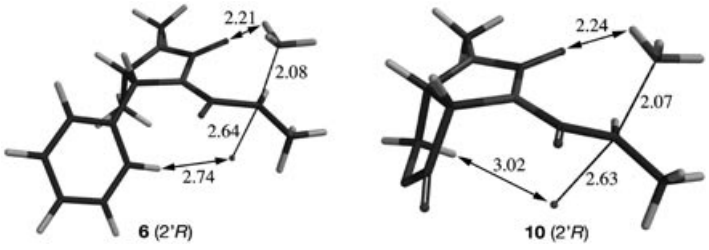

Figure 9. Transition state 3D models for structures **6** and **10**, epimers 2′*R*, at HF/6-31G**. Distances in Å.

of the hydrogen bond more difficult should increase the reaction final *de*. For instance, a structure type such as **11** (Table 4) could fulfil the requirement. We made the transition state modelling of some derivatives, but the results were not very promising, as it can be seen in Table 4.

Table 4. Transition state Gibbs energy differences (epimer 2′*R*−epimer 2′*S*) for three derivatives of **11** and theoretical diastereomeric excesses.

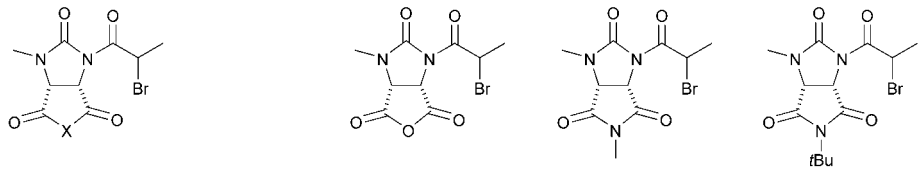

11 **12** **13** **14**

Method	$\Delta G^{\ddagger}_{2'R}-G^{\ddagger}_{2'S}$ [kJ mol^{-1}] and *de* [%]					
	12		**13**		**14**	
MP2/6-31G**//HF/6-31G**[a]	15.7	99.7	9.1	95.0	4.9	75.6
PW91/6-31G**[b]	13.5	99.2	9.8	96.3	7.6	91.2

[a] Scaling factor $a=1.58$. [b] Scaling factor $b=1.78$.

The oxygen derivative **12** was modelled only to compare the results with those obtained for compound **10** and also with the nitrogen derivatives **13** and **14**. Compound **12** is an anhydride and would not be possible to use it under the reaction conditions. Although compounds **13** and **14** are amides, it should be possible to use them. The results shown in Table 4 indicate that, in spite of a good result obtained for derivative **12**, lower diastereoisomeric excesses are expected for structures **13** and **14**. Nevertheless, we still consider that, due to their *meso* symmetry, they can be very interesting from an experimental point of view.

As it will be seen latter in the Experimental Section, derivatives of **10** were already prepared (structure **15**, Scheme 5) and tested as chiral auxiliaries. The results were not promising, since the auxiliary moieties react readily with the attacking amine to yield structures analogous of **16** (Scheme 5). The results, which indicate that compound **10** or its derivatives will not be useful as chiral auxiliaries, suggest a possible success of preparing analogous of **9** in a feasible process.

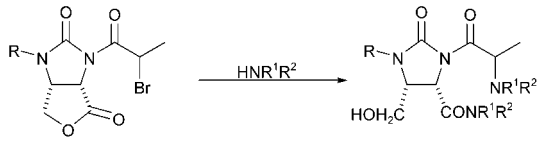

15 **16**

Scheme 5. Ester aminolysis of **15** (derivatives of **10**) when treated with primary or secondary amines in DKR conditions.

The behaviour of **15** (Scheme 5) was the main reason why we decided to calculate TS energies for several possible derivatives of **9** (structures **17** to **23**, Thable 5), expecting that the results could be extrapolated to the precursors of **16**. This approach simplifies the calculations, since all derivatives of **9** have less possible conformers than similar precursors of **16**. In two cases, which seemed interesting from an experimental point of view, we also calculated the precursors of **16** (structures **24** and **25**). The results are given in Table 5. The conclusion from these results is that, in all cases, there is a reduction in the expected *de* in comparison with compound **9**, with the values being close to those of compound **3**. Nevertheless we shall see in the Experimental Discussion that in order to get a reliable comparison of calculated relative energies, one has to reduce the scaling factors when applying them to structures **18** to **25**. In fact, compound **25** was prepared and tested in DKR reactions yielding diastereoisomeric excesses up to 99%. The best result found by Nunami for compound **3**, reacting with benzylamine as nucleophile, under the same experimental conditions we used was only 88%.[36] This means that structures **18** to **25** shall perform much better than indicated in Table 5. If a similar conclusion can be made for the amide structures **13** and **14** we can assume that the values in Table 4 are also underestimated. This makes these structures

Table 5. Transition state Gibbs energy differences (epimer 2′*R* - epimer 2′*S*) for derivatives of **9** and for two precursors of **16** and theoretical diastereomeric excesses.

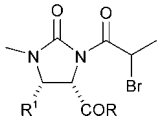

			$\Delta G^{\ddagger}_{2'R}-\Delta G^{\ddagger}_{2'S}$ [kJ mol^{-1}] and *de* [%]			
			MP2/6-31G**//HF/6-31G**[a]		PW91/6-31G**[b]	
17	R = OMe	R^1 = Me	16.8	99.8	16.8	99.8
18	R = NH_2	R^1 = Me	12.6	98.8	13.2	99.0
19	R = NMe_2	R^1 = Me	16.0	99.7	14.0	98.2
20	R = N(*i*Pr)$_2$	R^1 = Me	14.8	99.5	11.7	98.2
21	R = NH*t*Bu	R^1 = Me	12.4	98.6	12.5	98.7
22	R = NMe*t*Bu	R^1 = Me	15.3	99.6	13.5	99.2
23	R = Pyrrolidine	R^1 = Me	13.6	99.2	14.1	99.3
24	R = NH*t*Bu	R^1 = CH_2OMe	9.9	96.4	11.0	97.6
25	R = Pyrrolidine	R^1 = CH_2OMe	11.2	97.8	10.6	97.2

[a] Scaling factor $a=1.58$. [b] Scaling factor $b=1.78$.

even more interesting than suggested by the values in that Table.

We would finally like to analyze the behaviour of all calculated structures and try to understand the differences between them. Structures **10**, **12**, **13** and **14** have to be grouped together, since their fused ring system shows some particular aspects which are quite different from those of single ring structures. When we compare the structures in Figure 10

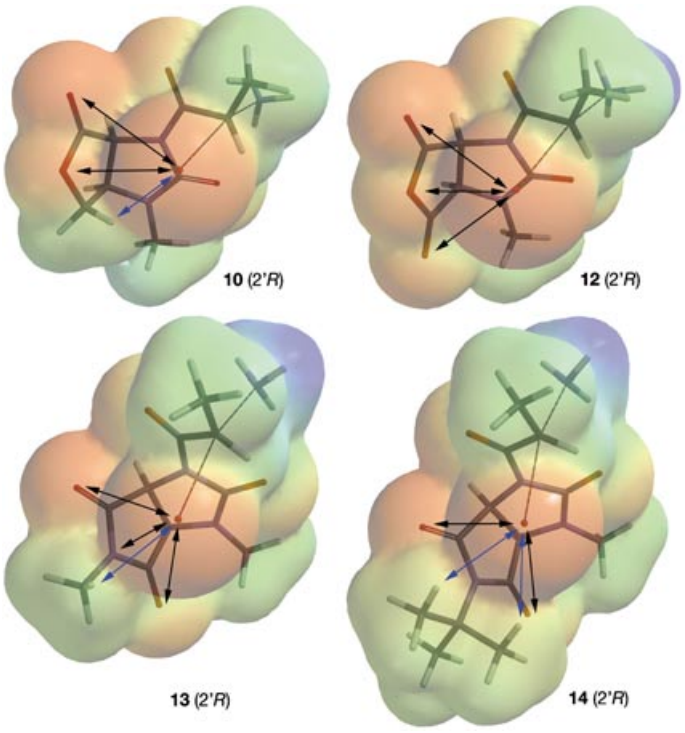

Figure 10. Electronic isodensity surfaces ($0.002\,e^{-}au^{-3}$, HF/6-31G**) mapped with the electrostatic potential, for TS structures of compounds **10**, **12**, **13** and **14** (2′*R* epimers), showing the electrostatic interactions (repulsive interactions: black arrows; attractive interactions: blue arrows) between the leaving bromide and the auxiliary substituent. Red zones indicate negative potential and blue zones indicate positive potential.

with the structures in Figure 8 we can see that, in all cases, the leaving bromide moves in the direction of the auxiliary ring. This movement forces the carbonyl group to move away (Figure 8) with rotation of the auxiliary substituent. In case of the structures in Figure 10 such a rotation is not possible. The leaving bromide still shows the same movement, reaching in the transition state a position near the oxygen or nitrogen atoms. The differences in electrostatic repulsion with these atoms are the major reason why structure **12** beaves better than structure **13**. Another effect is the electrostatic attraction between the leaving bromide and the methyl nitrogen group. This effect becomes very important when going to the least effective structure **14**. The result obtained for structure **10** (Table 3) when compared with the one for structure **12** (Table 4) indicates that, in spite of removing the hydrogen bond, the repulsive interaction is more strongly diminished, due to a removal of electron density from the central oxygen (anhydride system).

One could assume that since, in the transition state, the leaving bromide points away from the carbonyl oxygen atoms in structures **10** to **14**, the electrostatic interaction between them would not be as important. Nevertheless, we calculated the relative energies for structure **26** (Figure 11) showing that the change on the carbonyl position would reduce dramatically the performance of such an auxiliary.

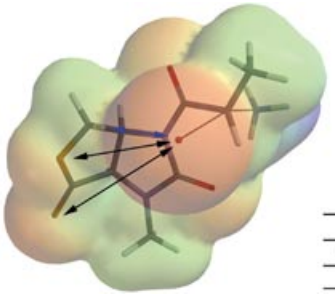

26

$\Delta G^{\ddagger}_{2'R}-\Delta G^{\ddagger}_{2'S}$ [kJ mol^{-1}] / *de* [%]			
MP2 6-31G**//HF 6-31G**[a]		PW91 6-31G**[b]	
4.3	69.5	2.0	37.9

Figure 11. Theoretical expected performance of structure **26** as a chiral auxiliary in DKR reactions, showing the electrostatic interactions in the transition state of epimer 2′*R* (repulsive interactions: black arrows; attractive interactions: blue arrows). (Electronic isodensity surfaces ($0.002\,e^{-}au^{-3}$, HF/6-31G**) mapped with the electrostatic potential. Red zones indicate negative potential and blue zones indicate positive potential.) Scaling factors: $a=1.58$ and $b=1.78$.

When we now compare the behaviour of structures **3**, **8**, **9** and structures **17** to **25**, we can see that the final outcome is a result of a very delicate equilibrium between repulsive and attractive electrostatic interactions. In these systems, since the bromine movement forces the rotation of the auxiliary substituent, any effect which reduces this rotation can increase the theoretical performance of the auxiliary in DKR reactions, as was stated before. For instance, when comparing structures **23** with **25**, one can see that there is a significant lowering of the *de* value. Since the only change is in the substituent in position 4, this change has to affect the behaviour of the substituent in position 3, in order to change the relative energies of both transition states. If one measures the rotation of the substituent in position 3, one can see that the dihedral angle in structure **23** is −72.7° while in **25** it is −76.7° (HF/6-31G**). This small change is due to a stronger polarization of the hydrogen atoms on the C-4 substituent, caused by the presence of the oxygen atom, which increases the electrostatic attraction with the carbonyl oxygen and decreases its electrostatic repulsion with the leaving bromide. A similar effect can be observed when comparing structures **21** and **24**.

In order to understand the relative importance of steric versus electrostatic interactions due to the substituent in C-4, we calculated the relative TS energies for structures **27** and **28**. The results are shown in Table 6 and suggest that the electrostatic repulsive interactions dictate the final relative energies. The steric hindrance caused by the CF_3 group

Table 6. Transition state Gibbs energy differences (epimer 2′*R*–epimer 2′*S*) for structures **27** and **28** and theoretical diastereomeric excesses.

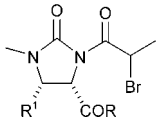

			$\Delta G^{\ddagger}_{2'R}-\Delta G^{\ddagger}_{2'S}$ [kJ mol^{-1}] and *de* [%]			
			MP2/6-31G**//HF/6-31G**[a]		PW91/6-31G**[b]	
27	R = *t*Bu	R^1 = *t*Bu	17.8	99.9	15.0	99.5
28	R = *t*Bu	R^1 = CF_3	23.8	99.99	19.7	99.9

[a] Scaling factor $a = 1.58$. [b] Scaling factor $b = 1.78$.

(structure **28**, Figure 12) has a value between the one due to a methyl group (structure **9**, Figure 12) and the one due to a *tert*-butyl group (structure **27**, Figure 12) but, in spite of this, the rotation of the C-3 substituent in structure **28** is only −19.2°, while in structure **27** it is −34.2° (compare the same rotation in structures **3** (−126.6°) and **9** (−70.8°)). Also, the expected *de* for structure **28** is quite higher, making it the best auxiliary for this kind of DKR reactions. We want to point out that these structures are optimised for DKR reactions where a bromide ion (or similar substituent) is the leaving group. We should not expect similar behaviours for reactions where electrostatic interactions are not as important as, for instance, in the addition reactions to double bonds. In such systems other factors shall be more important such as the steric or π–π interactions. In those cases, the substituents in the auxiliary have to be changed accordingly.

Experimental Discussion

Concerning the large number of possible chiral auxiliaries, we decided to take advantage of the availability of the imidazolidinone **29**, a substrate intermediate in the Hoffmann-La Roche synthesis of biotin[45] to synthesise the model substrate **10**. Initially we synthesised the analogue substrate **15** from **29** by partial deprotection (H_2/Pd/C/$HClO_4$) followed by acylation with 2-bromopropionyl bromide under our previously optimised conditions (Scheme 6).[46] When we submitted each separated epimer to nucleophilic substitution with benzylamine, the formation of a complex mixture was observed, from which we could isolate compounds **32** and **33**, resulting from competitive lactone ring opening and chiral auxiliary cleavage (Scheme 6). This result prompted us to synthesise the model chiral auxiliaries containing the carboxamide functional group in carbon C-5.

After several attempts to effect the short route based on selective benzyl deprotection, lactone ring opening and acylation of the resulted imidazolidinone unit, we ended up with the longer route presented in Scheme 7. After lactone ring opening with pyrrolidine and etherification of the hydroxyl group (AgO/MeI[47]), imidazo-

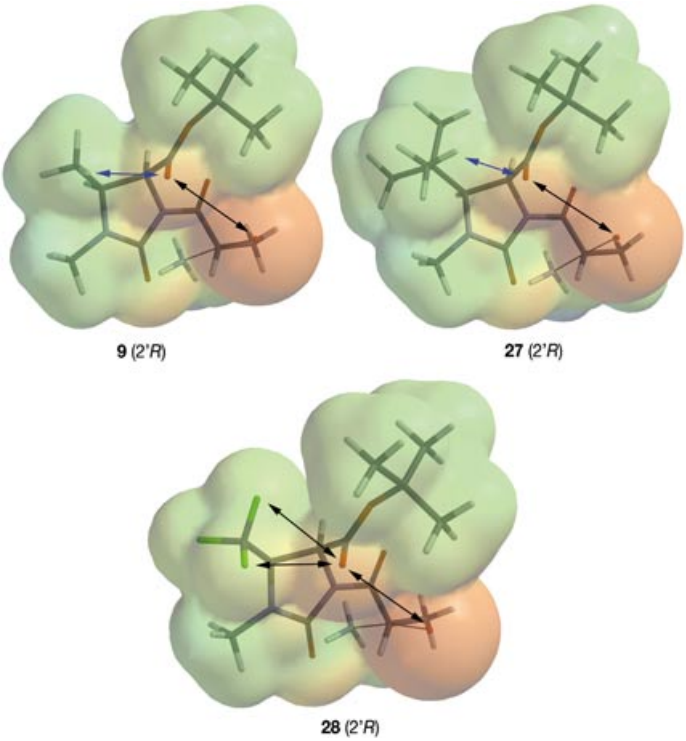

Figure 12. Electronic isodensity surfaces (0.002 e$^-$ au^{-3}, HF/6-31G**) mapped with the electrostatic potential, for TS structures of compounds **9**, **27** and **28** (2′*R* epimers), showing the electrostatic interactions (repulsive interactions: black arrows; attractive interactions: blue arrows) between the leaving bromide and the auxiliary substituent. Red zones indicate negative potential and blue zones indicate positive potential.

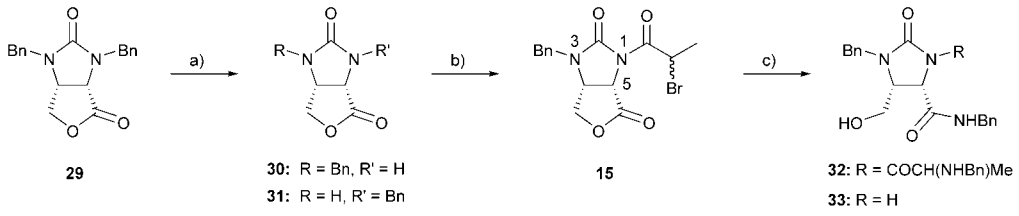

Scheme 6. Synthesis of the model substrate **15** and nucleophilic substitution attempts. a) Pd/C, H_2, $HClO_4$, MeOH, rt. b) 2,6-Lutidine, MeCHBrCOBr, CH_2Cl_2, −20 °C. c) Benzylamine (1.5 equiv), TEA (1.2 equiv), THF, rt, 48 h.

lidinone **34** was obtained, which originated **35** after hydrogenolysis (H_2/Pd/C/$HClO_4$). Several attempts to effect the monoalkylation, namely by prior selective N-H deprotonation, gave persistently the predominant alkylation in the undesired N-1 position. To circumvent this reactivity, **35** was monobenzylated (NaH/BnBr) to give a mixture of **36** and **37** in a 87:13 ratio, which was followed by methylation (NaH/MeI) and benzyl deprotection (H_2/Pd/C/$HClO_4$) to give a mixture of **40** and **41**. Acylation of this mixture under reported conditions (*t*BuOK/MeCHBrCOBr)[48] gave the isomers **42** and **43** which were separated by chromatography.

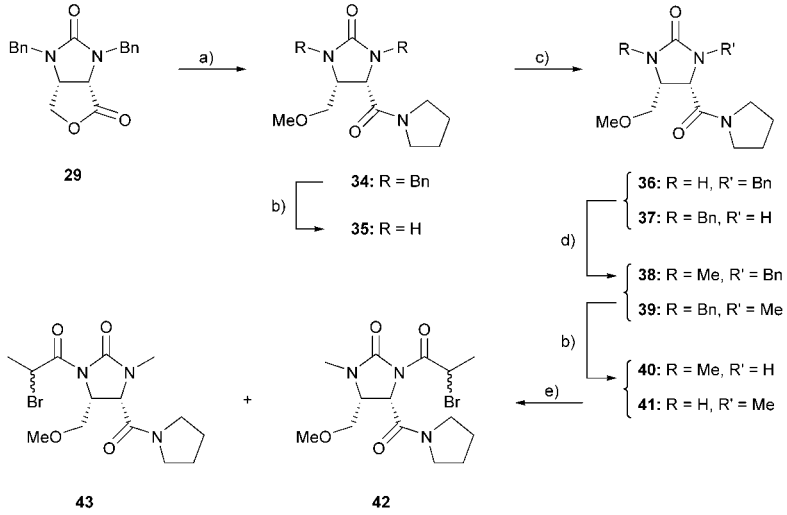

Scheme 7. Synthesis of the model substrate **42**. a) i) pyrrolidine (1.5 equiv), CH_2Cl_2, rt, 24 h; ii) AgO (1.5 equiv), MeI (excess), MeCN, 40 °C, 3 d, 59 %. b) Pd/C, H_2, $HClO_4$, MeOH, rt, quantitative. c) NaH (0.5 mol equiv), BnBr (0.5 mol equiv), THF, 0 °C to rt, 3 h, 35 %. d) NaH (0.5 mol equiv), MeI (1.0 equiv), THF, 0 °C to rt, 3 h, 91 %. e) *t*BuOK (1.0 equiv), THF, MeCHBrCOBr (1.4 equiv), −50 to −30 °C, 87 %.

By using an 1:1 epimeric mixture of **42**, several nucleophilic substitutions with benzylamine were tested (Table 7). Under the same DKR conditions described before for substrate **6**, using Bu_4NBr, we were pleased to observe that the substitution occurs quantitatively and in a very high diastereoselectivity (entry 1, *de* 99 %). These results have to be compared with the ones obtained for substrate **6** under identical experimental conditions (*de* 58 %)[41] and also with the one for substrate **3** (*de* 88 %).[36] In case of BuNI the yield is also high and, more important, we were unable to detect by HPLC the minor epimer of **44** (entry 2) while in case of substrate **6** moderate diastereoselectivity was observed (*de* 74 %).[41] In order to afford enough quantity of the minor epimer of **44** for characterization purposes and HPLC standard, the reaction was performed in the presence of $AgNO_3$ giving **44** and the corresponding epimer as the minor product but in lower stereocontrol (*de* 56 %, entry 3). To determine the absolute configuration of product **44**, we prepared the corresponding methyl ester, by removing the chiral auxiliary via methanolysis. The resulting enantiomeric mixture was analysed by chiral-phase HPLC and was compared with a sample of the same compound, prepared by using substrate **7**, following the literature procedure.[41] We determined that the major product obtained in our reaction is, as expected, (*R*)-methyl 2-(benzylamino)-propionate. All these results clearly show that there is a very high difference in reactivity between both epimers, which are in accordance with the molecular modelling predictions. These results give strong support for the idea that similar experimental stereocontrol should be obtained for the other structures presented in Table 5, allowing the possibility to develop other more efficient chiral auxiliaries, which should also be more easily synthesized.

Conclusion

Since both imidazolidinones and oxazolidinones are used as chiral auxiliaries in a large number of different types of reactions, understanding their behaviour is still a very important matter. Numerous papers are known where the rationalization of the performance of this type of auxiliaries was mainly based in the idea that the two carbonyl groups can be in a parallel or antiparallel conformation, usually depending on the coordination with a Lewis acid. Here, we reinforce the idea that this is not necessarily true, proposing an alternative mecha-

Table 7. Nucleophilic substitution on **42** with benzylamine (1:1 mixture of epimers).

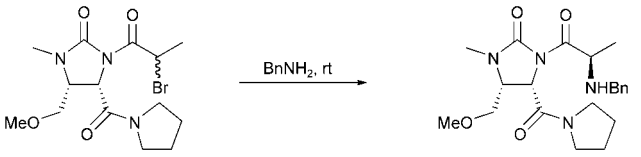

	Conditions	Yield [%]	*de* [%][a]	Reported *de* [%] **6**[b]	**3**[c]
1	$BnNH_2$ (1.5 equiv), nBu_4NBr (0.2 equiv) TEA (1.2 equiv), THF, rt, 48 h	quant.	99	58	88
2	$BnNH_2$ (1.5 equiv), nBu_4NI (0.2 equiv) TEA (1.2 equiv), THF, rt, 48 h	92	100	74	
3	$BnNH_2$ (3.0 equiv), $AgNO_3$ (2.0 equiv) THF, rt, 48 h	97	56		

[a] *de* determined by HPLC. [b] Reported *de* under identical experimental conditions for substrate **6**.[41] [c] Reported *de* under different experimental conditions (TEA, HMPA, rt) for substrate **3**.[36]

nism and also new molecules with optimized performance. Our proposed mechanism was experimentally tested yielding very good results which opens the door to the idea that similar explanations can be acceptable for other reaction types, where performance enhancement shall also be reached, based in simple but efficient structural modifications.

Experimental Section

General methods: THF was distilled over calcium hydride immediately before use, while triethylamine and dichloromethane were freshly distilled over calcium hydride and P_2O_5, respectively. Sodium hydride was used as a 55% dispersion in mineral oil. All reactions were performed in oven-dried glassware under an atmosphere of argon. Flash chromatography was carried out on silica gel 60M from Macherey–Nagel (no. 815381). Reaction mixtures were analysed by TLC by using ALUGRAM SIL G/UV_{254} from MN (no. 818133, silica gel 60). Visualisation of TLC spots was effected using UV and solution of phosphomolybdic acid or I_2. The melting points were determined with an Electrothermal Mod. IA6304 in capillary tubes and are uncorrected. The diastereomeric ratio of **44** was determined by HPLC analysis using Dionex components P680, UVD340S on a Chiralpak AD column (0.46 cm, 25 cm) at 25°C. IR spectra were recorded by using a Mattson Instruments, model Satellite FTIR, as thinly dispersed films and, unless otherwise stated, are quoted in cm^{-1}. High and low resolution mass spectra (EI, FAB) were carried out by Mass Spectrometry Service at the University of Santiago de Compostela (Spain). The microanalyses were carried out by the CQFB analytical service using a CHNS Analyser Thermo Finnigan model Flash 1112. NMR spectra were recorded in a Bruker AMX 400 using $CDCl_3$ as solvent (unless otherwise stated) and $(CH_3)_4Si$ (^1H) as internal standard. Chemical shifts are expressed in ppm and coupling constants in Hz. The assignment of the signals in the NMR spectra of the compounds were based on their characteristic chemical shifts, multiplicity and, when necessary, by 2D NMR techniques (COSY and HMQC).

Preparation of 30 and 31 by partial hydrogenation of lactone 29: A solution of **29** (2.00 g, 6.20 mmol), 60% perchloric acid (0.4 mL, 4.0 mmol), and 10 wt.% palladium on charcoal (500 mg, 0.5 mmol Pd) in MeOH (290 mL) was hydrogenated at 40 psi for a period of 2 d at room temperature. The catalyst was removed by filtration and the solution was neutralized with solid $NaHCO_3$. After filtration of the latter, the crude reaction mixture was subjected to a column chromatography (70% ethyl acetate/hexane to pure ethyl acetate) to yield **29** (107 mg, 5%), **30** (205 mg, 10%) and **31** (136 mg, 6%), while the fully unprotected product remained on the silica gel.

Compound 30: white needles; m.p. 133–134°C (hexane/ethyl acetate); $[\alpha]_D = +67°$ ($c = 1.2$, $CHCl_3$); ^1H NMR ($CDCl_3$): $\delta = 7.37–7.24$ (m, 5H, Ph), 4.68 (d, $J = 15.4$ Hz, 1H, $^1/_2$ of Ph-CH_2), 4.31–4.19 (m, 5H, $^1/_2$ of Ph-CH_2 + CH + CH + OCH_2); ^{13}C NMR ($CDCl_3$): $\delta = 174.7$ (*C*O), 159.7 (*C*O), 135.6 (*i*Ph), 129.0 (Ph), 128.1 (Ph), 69.8 (O*C*H$_2$), 56.2 (CH), 51.2 (CH), 46.0 (*C*H$_2$Ph); IR: $\tilde{\nu} = 3254$, 3088, 2969, 2923, 1782, 1701, 1447, 1421, 1216, 1025, 975, 758, 706 cm^{-1}; MS (EI): *m*/*z* (%): 232 (68) $[M]^+$, 174 (9) $[M-COOCH_2]^+$, 147 (41), 132 (28), 91 (100) $[PhCH_2]^+$; HRMS (EI+): *m*/*z*: calcd for $C_{12}H_{12}N_2O_3$: 232.084792; found: 232.085448.

Compound 31: white needles; m.p. 160–161°C (hexane/ethyl acetate); $[\alpha]_D = +97°$ ($c = 1.2$, $CHCl_3$); ^1H NMR ($CDCl_3$): $\delta = 7.39–7.31$ (m, 5H, Ph), 4.90 (d, $J = 15.0$ Hz, 1H, $^1/_2$ of Ph-CH_2), 4.50–4.38 (m, 3H, CH_2CH + OCH_2), 4.35 (d, $J = 15.0$ Hz, 1H, $^1/_2$ of Ph-CH_2), 4.05 (d, $J = 8.4$ Hz, 1H, COCH); ^{13}C NMR ($CDCl_3$): $\delta = 172.8$ (*C*O), 160.2 (*C*O), 135.6 (*i*Ph), 128.8 (Ph), 128.6 (Ph), 127.9 (Ph), 73.5 (O*C*H$_2$), 54.7 (CO*C*H), 50.8 (CH_2CH), 44.5 (*C*H$_2$Ph); IR:$\tilde{\nu} = 3289$, 3030, 2970, 2923, 1772, 1699, 1450, 1427, 1363, 1244, 1216, 1178, 996, 754, 715 cm^{-1}; MS (EI): *m*/*z* (%): 232 (40) $[M]^+$, 188 (5) $[M-CO_2]^+$, 174 (17) $[MCOOCH_2]^+$, 97 (31), 91 (100) $[PhCH_2]^+$, 58 (53); HRMS (EI+): *m*/*z*: calcd for $C_{12}H_{12}N_2O_3$: 232.084792; found: 232.085885.

Preparation of 15: 2-Bromopropionyl bromide (190 μL, 1.81 mmol) was added to a stirred solution of **30** (278 mg, 1.20 mmol) and 2,6-lutidine (200 μL, 1.72 mmol) in CH_2Cl_2 (15 mL) at −20°C, and the reaction mixture was stirred at −20°C for 2 h. The solution was allowed to reach the room temperature, washed with aqueous NH_4Cl and dried with $MgSO_4$. The solvent was evaporated and the residue was purified by column chromatography (20% ethyl acetate/hexane to pure ethyl acetate) to yield in order of elution **15a** (less polar epimer, 77 mg, 21.0%), **15b** (more polar epimer, 76 mg, 20.8%) and recovered starting material **30** (105 mg, 37.8%).

Compound 15a: white needles; m.p. 181–182°C (hexane/ethyl acetate); $[\alpha]_D = -106°$ ($c = 0.55$, $CHCl_3$); ^1H NMR ($CDCl_3$): $\delta = 7.39–7.25$ (m, 5H, Ph), 5.81 (q, $J = 6.8$ Hz, 1H, CHBr), 5.24 (d, $J = 5.6$ Hz, 1H, COCH), 4.84 (d, $J = 15.2$ Hz, 1H, $^1/_2$ of Ph-CH_2), 4.39–4.27 (m, 4H, $^1/_2$ of Ph-CH_2 + CH_2CH + OCH_2), 1.88 (d, $J = 6.8$ Hz, 3H, CH_3); ^{13}C NMR ($CDCl_3$): $\delta = 171.2$ (CO), 168.8 (CO), 152.6 (CO), 134.1 (*i*Ph), 129.3 (Ph), 128.6 (Ph), 128.0 (Ph), 67.2 (O*C*H$_2$), 53.6 (CH), 52.5 (CH), 46.1 (Ph*C*H$_2$), 39.3 (CHBr), 20.7 (CH_3); IR: $\tilde{\nu} = 3030$, 2980, 2927, 1791, 1738, 1699, 1376, 1206, 1155, 1024 cm^{-1}; elemental analysis calcd (%) for $C_{15}H_{15}BrN_2O_4$: C 49.06, H 4.12, N 7.63; found: C 48.74, H 4.10, N 7.30.

Compound 15b: white needles; m.p. 185–186.5°C (hexane/ethyl acetate); $[\alpha]_D = -115°$ ($c = 0.31$, $CHCl_3$); ^1H NMR ($CDCl_3$): $\delta = 7.39–7.24$ (m, 5H, Ph), 5.80 (q, $J = 6.0$ Hz, 1H, CHBr), 5.30 (d, $J = 6.8$ Hz, 1H, COCH), 4.83 (d, $J = 15.3$ Hz, 1H, $^1/_2$ of Ph-CH_2), 4.39–4.27 (m, 4H, $^1/_2$ of Ph-CH_2 + CH_2CH + OCH_2), 1.86 (d, $J = 6.0$ Hz, 3H, CH_3); ^{13}C NMR ($CDCl_3$): $\delta = 170.4$(CO), 168.9(CO), 152.6 (CO), 134.1 (*i*Ph), 129.4(Ph), 128.7(Ph), 128.4(Ph), 67.4 (O*C*H$_2$), 53.4 (CH), 51.9 (CH), 46.3 (Ph*C*H$_2$), 38.5 (*C*HBr), 20.3 (CH_3); IR: $\tilde{\nu} = 3030$, 2986, 2932, 1791, 1737, 1695, 1411, 1375, 1323, 1208, 1155, 985 cm^{-1}; elemental analysis calcd (%) for $C_{15}H_{15}BrN_2O_4$: C 49.06, H 4.12, N 7.63; found C 48.77, H 4.10, N 7.62.

Substitution reaction of 15a with benzylamine: Benzylamine (67 μL, 3 equiv) was added at room temperature to a stirred solution of **15a** (77 mg, 0.21 mmol) in THF (0.7 mL). After 48 h the solvent was evaporated and the crude reaction mixture was purified by column chromatography (60% ethyl acetate/hexane to pure ethyl acetate) to yield a complex mixture (21 mg) from which the product **32** was obtained by crystallization from ethanol, white plates. M.p. 201–202°C; ^1H NMR ([D$_6$]DMSO): $\delta = 7.35–7.21$ (m, 15H, Ph), 5.04 (t, $J = 4.1$ Hz, 1H), 4.79 (d, $J = 9.4$ Hz, 1H), 4.61 (d, $J = 15.7$ Hz, 1H), 4.53 (q, $J = 6.7$ Hz, 1H, CHCH$_3$), 4.43 (m, 2H), 4.23 (dd, $J = 15.3$, 5.0 Hz, 1H), 3.85–3.41 (signals overlapped with water), 1.18 (d, $J = 6.6$ Hz, 3H, CH_3); ^{13}C NMR ([D$_6$]DMSO): $\delta = 176.6$ (CO), 167.3 (CO), 155.1 (CO), 140.8 (*i*Ph), 139.2 (*i*Ph), 137.5 (*i*Ph), 128.9 (Ph), 128.7 (Ph), 128.6 (Ph), 127.84 (Ph), 127.8 (Ph), 127.6 (Ph), 127.3 (Ph), 127.4 (Ph), 60.4 (O*C*H$_2$), 56.6 (CH), 55.7 (CH), 54.6 (CH), 50.9 (*C*H$_2$Ph), 45.9 (*C*H$_2$Ph), 40.4 (*C*H$_2$Ph), 19.5 (*C*H$_3$); IR (KBr): $\tilde{\nu} = 3292$, 3109, 3024, 2933, 2843, 1724, 1686, 1661, 1568, 1453, 1421, 1399, 1324, 1247, 1227, 1063, 748, 738, 700 cm^{-1}; MS (CI): *m*/*z* (%): 501 (1) $[M+H]^+$, 394 (3) $[M-NHCH_2Ph]$, 340 (10) $[M-COCH(CH_3)NHCH_2Ph]^+$, 233 (41), 205 (13), 175 (13), 134 (68) $[CONHCH_2Ph^+]^+$, 119 (25) $[PhCH_2NHCH]^+$, 106 (63) $[NHCH_2Ph]^+$, 91 (100) $[PhCH_2]^+$; HRMS (CI+): *m*/*z*: calcd for $C_{29}H_{33}N_4O_4$: 501.250181; found: 501.249859.

Substitution reaction of 15b with benzylamine: Benzylamine (67 μL, 3 equiv) was added at room temperature to a stirred solution of **15b** (76 mg, 0.21 mmol) in THF (0.7 mL). After 48 h the solvent was evaporated and the crude reaction mixture was purified by preparative TLC (ethyl acetate) to yield **33** (55 mg) with some impurities that were removed by crystallization in ethyl acetate, white plates. M.p. 201–202°C; ^1H NMR ([D$_6$]DMSO): $\delta = 7.34–7.23$ (m, 10H, Ph), 4.82 (t, $J = 4.9$ Hz, 1H), 4.57 (d, $J = 15.7$ Hz, 1H), 4.29 (d, $J = 5.6$ Hz, 2H), 4.16 (d, $J = 15.7$ Hz, 1H), 4.13 (d, $J = 10.1$ Hz, 1H), 3.67–3.48 (signals overlapped with water); ^{13}C NMR ([D$_6$]DMSO): $\delta = 170.1$ (CO), 162.2 (CO), 139.4 (*i*Ph), 138.5 (*i*Ph), 128.8 (Ph), 128.7 (Ph), 128.0 (Ph), 127.9 (Ph), 127.4 (Ph), 127.3 (Ph), 60.4 (O*C*H$_2$), 58.4 (CH), 55.4 (CH), 45.4 (*C*H$_2$Ph), 42.8 (*C*H$_2$Ph); IR (KBr): $\tilde{\nu} = 3391$, 3298, 2930, 1711, 1670, 1649, 1550, 1474,

1454, 1252, 1082, 1070, 1058, 1044, 1030, 701; MS (IE): *m/z* (%): 339 (1) $[M]^+$, 308 (2) $[M-CH_2OH]^+$, 232 (6), 205 (10) $[M-CONHCH_2Ph]^+$, 175 (60) $[M-CH_2OH\text{-}CONHCH_2Ph]^+$, 106 (9) $[NHCH_2Ph]^+$, 91 (100) $[PhCH_2]^+$; HRMS (EI+): *m/z*: calcd for $C_{19}H_{21}N_3O_3$: 339.158292; found: 339.159463.

Preparation of 34: Pyrrolidine (2 mL, 24 mmol) was added to a stirred solution of **29** (5.07 g, 15.7 mmol) in CH_2Cl_2 (30 mL). The solution was stirred at room temperature for 24 h, and then washed consecutively with an aqueous HCl (1 M) solution and brine. After drying with $MgSO_4$, the organic phase was evaporated. The white solid compound was dissolved in acetonitrile (15 mL), and then Ag_2O (5.5 g, 24 mmol) and CH_3I (6 mL) were added. The reaction mixture was stirred under argon atmosphere for 3 d at 40 °C and after filtration, the crude reaction mixture was diluted with CH_2Cl_2 and washed with 10% aq. ammonia. The organic phase was dried with $MgSO_4$, evaporated and the residue was purified by column chromatography (80% ethyl acetate/hexane), after which the product **34** (3.77 g, 59%) was obtained as an oil. $[\alpha]_D = +12°$ (*c* = 1.1, $CHCl_3$); ^{1}H NMR ($CDCl_3$): δ = 7.32–7.21 (m, 10H, Ph), 5.04 (d, *J* = 14.5 Hz, 1H, $^1/_2$ of Ph-CH_2), 4.66 (d, *J* = 15.7 Hz, 1H, $^1/_2$ of Ph-CH_2), 4.25 (d, *J* = 15.7 Hz, 1H, $^1/_2$ of Ph-CH_2), 4.00 (d, *J* = 9.3 Hz, 1H, C*H*-CO-Py), 3.84 (d, *J* = 14.5 Hz, 1H, $^1/_2$ of Ph-CH_2), 3.69 (m, 1H, C*H*-CH_2OMe), 3.38–3.51 (m, 3H, $^1/_2$ of CH_2NCH_2 + $^1/_2$ of CH_2OMe), 3.30 (t, *J* = 8.9 Hz, 1H, $^1/_2$ of CH_2OMe), 3.11 (m, 1H, $^1/_4$ of CH_2NCH_2), 3.12 (s, 3H, OCH_3), 2.60 (m, 1H, $^1/_4$ of CH_2NCH_2), 1.73 (m, 4H, CH_2CH_2NCH_2CH_2); ^{13}C NMR ($CDCl_3$): δ = 165.6 (*C*O), 160.4 (*C*O), 137.6 (*i*Ph), 136.3 (*i*Ph), 128.7 (Ph), 128.4 (Ph), 127.7 (Ph), 127.6 (Ph), 127.2 (Ph), 70.3 (*C*H_2OMe), 58.7 (OCH_3), 56.0 (CH), 54.0 (CH), 46.6 (CH_2), 46.0 (CH_2), 45.7 (CH_2), 25.9 (NCH_2CH_2), 23.4 (NCH_2CH_2); IR: $\tilde{\nu}$ = 3062, 3029, 2973, 2927, 2875, 1699, 1649, 1447, 1358, 1237, 1130, 1099, 703 cm^{-1}; MS (EI): *m/z* (%): 408 (2) $[M+H]^+$, 375 (4) $[M-MeOH]^+$, 362 (2) $[M-MeOCH_2]^+$, 309 (25) $[M-COPy]^+$, 98 (25), 91 (100) $[PhCH_2]^+$, 55 (25); HRMS (EI+): *m/z*: calcd for $C_{24}H_{29}N_3O_3$: 407.220892; found: 407.219322.

Preparation of 35: A solution of **34** (3.479 g, 8.5 mmol), 60% perchloric acid (0.4 mL, 4.0 mmol), and 10 wt.% palladium on charcoal (1.03 g, 1 mmol Pd) in MeOH (200 mL) was hydrogenated at 65 psi for a period of 4 d at room temperature. The catalyst was removed by filtration and the solution was neutralized with solid $NaHCO_3$. After filtration of the latter, the crude reaction mixture was subjected to a column chromatography (10% MeOH/CH_2Cl_2) and the product **35** was obtained in a quantitative yield as a white solid. $[\alpha]_D = -45°$ (*c* = 1.4, $CHCl_3$); ^{1}H NMR ($CDCl_3$): δ = 4.73 (d, *J* = 9.3 Hz, 1H, C*H*-CO-Py), 4.21 (m, 1H, C*H*-CH_2OMe), 3.61 (m, 1H, $^1/_4$ of CH_2NCH_2), 3.50–3.27 (m, 5H, 3 H of CH_2NCH_2 + CH_2OMe), 3.50 (s, 3H, OCH_3), 2.03–1.83 (m, 4H, CH_2CH_2NCH_2CH_2); ^{13}C NMR ($CDCl_3$): δ = 167.9 (*C*O), 164.5 (*C*O), 71.5 (*C*H_2OMe), 59.0 (OCH_3), 55.9 (*C*H-CO-Py), 53.4 (*C*H-CH_2OMe), 46.4 (NCH_2), 46.2 (NCH_2), 26.0 (NCH_2CH_2), 23.9 (NCH_2CH_2); IR: $\tilde{\nu}$ = 3385, 2976, 2930, 2882, 1695, 1632, 1455, 1343, 1268, 1196, 1097 cm^{-1}; MS (EI): *m/z* (%): 227 (2) $[M]^+$, 195 (6) $[M-MeOH]^+$, 182 (7) $[M-MeOCH_2]^+$, 129 (53) $[M-COPy]^+$, 99 (88), 98 (100), 84 (26), 70 (58), 56 (38), 55 (43); HRMS (EI+): *m/z*: calcd for $C_{10}H_{17}N_3O_3$: 227.126992; found: 227.126997.

Preparation of 36 and 37: A solution of compound **35** (2.40 g, 11 mmol) in dry THF (10 mL) was added to a stirred suspension of NaH (60% in oil, 260 mg, 6.5 mmol) in dry THF (40 mL) at 0 °C. The mixture was stirred for 10 min at 0 °C, and afterwards benzylbromide (770 μL, 6.5 mmol) was added, and the stirring was continued at room temperature for 3 h. The solvent was evaporated and the crude reaction mixture was purified by column chromatography (ethyl acetate to 20% MeOH/CH_2Cl_2) to obtain a mixture of isomers **36** and **37** (1.22 g, 35%, 70% based on limiting NaH) in 87:13 ratio (determined by NMR). A small sample of this mixture was subjected to preparative TLC (3% MeOH/CH_2Cl_2) and after several developments the major product **36** was isolated and characterised.

Compound 36: ^{1}H NMR ($CDCl_3$): δ = 7.30–7.18 (m, 5H, Ph), 5.00 (d, *J* = 14.5 Hz, $^1/_2$ of Ph-CH_2), 4.13 (d, *J* = 8.9 Hz, 1H, C*H*-CO-Py), 3.87 (d, *J* = 14.5 Hz, 1H, $^1/_2$ of Ph-CH_2), 3.87 (m, 1H, C*H*-CH_2OMe), 3.52 (m, 1H, $^1/_4$ of CH_2NCH_2), 3.46–3.37 (m, 2H, $^1/_4$ of CH_2NCH_2 + $^1/_2$ of CH_2OMe), 3.29 (m, 1H, $^1/_2$ of CH_2OMe), 3.26 (s, 3H, OCH_3), 3.14 (m, 1H, $^1/_4$ of CH_2NCH_2), 2.82 (m, 1H, $^1/_4$ of CH_2NCH_2), 1.81 (m, 4H, CH_2CH_2NCH_2CH_2); ^{13}C NMR ($CDCl_3$): δ = 164.8 (*C*O), 161.0 (*C*O), 135.9 (*i*Ph), 128.8 (Ph), 128.6 (Ph), 127.7 (Ph), 72.0 (*C*H_2OMe), 59.0 (OCH_3), 57.3 (*C*H-CO-Py), 50.4 (*C*H-CH_2OMe), 46.1 (NCH_2), 45.7 (*C*H_2Ph + NCH_2), 26.0 (NCH_2CH_2), 23.9 (NCH_2CH_2); IR: $\tilde{\nu}$ = 3265, 2921, 2851, 1702, 1642, 1451, 1343, 1254, 1128, 1097, 704 cm^{-1}; MS (FAB+): *m/z* (%): 318 (34) $[M+H]^+$, 231 (49), 155 (19), 154 (89), 137 (100), 109 (47); HRMS (FAB+): *m/z*: calcd for $C_{17}H_{24}N_3O_3$: 318.181767; found: 318.181607.

Partial spectral data obtained for **37** from the mixture of **36** and **37**: ^{1}H NMR ($CDCl_3$): δ = 4.75 (d, *J* = 15.5 Hz, 1H, $^1/_2$ of Ph-CH_2), 4.50 (d, *J* = 9.0 Hz, 1H, C*H*-CO-Py), 4.13 (d, *J* = 15.5 Hz, 1H, $^1/_2$ of Ph-CH_2), 3.18 (s, 3H, OCH_3); ^{13}C NMR ($CDCl_3$): δ = 137.3 (*i*Ph), 70 (*C*H_2OMe).

Preparation of 38 and 39: A solution of a mixture of **36** and **37** (1.51 g, 4.76 mmol) in dry THF (10 mL) was added at 0 °C to a stirred suspension of NaH (60% in oil, 190 mg, 4.76 mmol) in dry THF (30 mL). The reaction mixture was stirred for 10 min at 0 °C, and afterwards CH_3I (0.3 mL, 4.76 mmol) was added, and the stirring was continued at room temperature for 2 h. The mixture was diluted with CH_2Cl_2, washed with aq NH_4Cl, and dried with $MgSO_4$. After evaporation, the residue was purified by column chromatography (3% MeOH/CH_2Cl_2) and a mixture of regioisomers **38** and **39** (1.43 g, 91%) was obtained.

^{1}H NMR (the number of the protons is calculated with respect to the integral of the peak at 4.30 for the minor and at 4.07 for the major product **38**): δ = 7.33–7.21 (m, Ph of both isomers), 4.98 (d, *J* = 14.5 Hz, 1H, $^1/_2$ of Ph-CH_2^{major}), 4.69 (d, *J* = 15.3 Hz, 1H, $^1/_2$ of Ph-CH_2^{minor} **39**), 4.30 (d, *J* = 8.9 Hz, 1H, C*H*-CO-Py^{minor}), 4.19 (d, *J* = 15.3 Hz, 1H, $^1/_2$ of Ph-CH_2^{minor}), 4.07 (d, *J* = 8.9 Hz, 1H, C*H*-CO-Py^{major}), 3.82 (d, *J* = 14.5 Hz, 1H, $^1/_2$ of Ph-CH_2^{major}), 3.71 (m, 1H, C*H*-CH_2OMe), 3.60–3.22 (m, CH_2OMe + $^3/_4$ of CH_2NCH_2 of both isomers), 3.25 (s, 3H, OCH_3^{major}), 3.17 (s, 3H, OCH_3^{minor}), 2.83 (s, 3H, NCH_3^{major}), 2.79 (s, 3H, NCH_3^{minor}), 2.72 (m, $^1/_4$ of CH_2NCH_2 of both isomers), 1.81 (m, CH_2CH_2NCH_2CH_2 of both isomers); ^{13}C NMR ($CDCl_3$): δ = 165.8 (CO^{minor}), 165.6 (CO^{major}), 160.4 (CO), 137.4 (*i*Ph^{minor}), 136.3 (*i*Ph^{major}), 128.8 (Ph), 128.4 (Ph), 127.8 (Ph), 127.5 (Ph), 127.2 (Ph), 70.1 (*C*H_2OMe^{major}), 69.8 (*C*H_2OMe^{minor}), 58.8 (OCH_3), 56.5 (CH), 56.1 (CH), 46.4 (CH_2), 46.2 (CH_2), 46.0 (CH_2), 45.7 (CH_2), 30.0 (NCH_3^{major}), 29.8 (NCH_3^{major}), 26.1 (NCH_2CH_2^{minor}), 26.0 (NCH_2CH_2^{major}), 23.9 (NCH_2CH_2); IR: $\tilde{\nu}$ = 2971, 2927, 2877, 1696, 1647, 1449, 1403, 1342, 1245, 1098, 704 cm^{-1}; MS (EI): *m/z* (%): 332 (2) $[M+H]^+$, 299 (6) $[M-MeOH]^+$, 233 (31) $[M-COPy]^+$, 98 (35), 91 (100) $[PhCH_2]^+$, 56 (23), 55 (30); HRMS (EI+): *m/z*: calcd for $C_{18}H_{25}N_3O_3$: 331.189592; found: 331.188348.

Preparation of 40 and 41: A solution of **38** and **39** (1.43 g, 4.32 mmol), 60% perchloric acid (0.1 mL, 1 mmol), and 10 wt.% palladium on charcoal (500 mg, 0.5 mmol) in MeOH (100 mL) was hydrogenated at 65 psi for a period of 18 h. The catalyst was removed by filtration and the solution was neutralized with solid $NaHCO_3$. After filtration of the latter, the crude reaction mixture was subjected to a column chromatography (3% MeOH/CH_2Cl_2) and a mixture of isomers **40** and **41** was obtained in quantitative yield as a white solid.

^{1}H NMR (the number of the protons is calculated with respect to the integral of the peak at 4.37 for the minor and at 4.51 for the major product): δ = 4.51 (d, *J* = 9.3 Hz, 1H, C*H*-CO-Py^{major}), 4.37 (d, *J* = 9.3 Hz, 1H, C*H*-CO-Py^{minor}), 3.84–3.99 (m, C*H*-CH_2OMe of both isomers), 3.21–3.48 (m, CH_2OMe + CH_2NCH_2 of both isomers), 3.18 (s, OCH_3 of both isomers), 2.69 (s, 3H, NCH_3^{major}), 2.62 (s, 3H, NCH_3^{minor}), 1.72–1.90 (m, CH_2CH_2N CH_2CH_2 of both products); ^{13}C NMR ($CDCl_3$): δ = 167.5 (CO), 165.4 (CO^{minor}), 161.9 (CO), 71.7 (*C*H_2OMe^{minor}), 69.7 (*C*H_2OMe^{major}), 61.4 (*C*HCOPy^{minor}), 58.9, 58.7, 54.2 (*C*HCOPy^{major}), 50.2 (*C*HCH$_2$OMe^{minor}), 46.4 (NCH_2^{major}), 46.2 (NCH_2^{minor}), 46.0 (NCH_2^{major}), 45.9 (NCH_2^{minor}), 29.3 (NCH_3^{minor}), 29.1 (NCH_3^{major}), 26.1 (NCH_2CH_2^{minor}), 26.0 (NCH_2CH_2^{major}), 24.0 (NCH_2CH_2^{minor}), 23.9 (NCH_2CH_2^{major}); IR: $\tilde{\nu}$ = 3419, 2975, 2934, 2884, 1690, 1634, 1455, 1407, 1344, 1262, 1193, 1095, 624 cm^{-1}; MS (EI): *m/z* (%): 241 (2) $[M]^+$, 209 (4) $[M-MeOH]^+$, 143 (39) $[M-COPy]^+$, 113 (53), 98 (100), 70 (27), 56 (37), 55 (52); HRMS (EI+): *m/z*: calcd for $C_{11}H_{19}N_3O_3$: 241.142642; found: 241.143564.

Preparation of 42: Potassium *tert*-butoxide (424 mg, 3.78 mmol) was added to a solution of a mixture of isomers **40** and **41** (910 mg, 3.78 mmol) in THF (10 mL) at −50 °C with stirring under argon atmosphere. After 20 min, 2-bromopropionyl bromide (640 μL, 5.29 mmol) was added, and stirring was continued for another hour at −30 °C. Dichloromethane was added and the reaction mixture was washed with aq NH_4Cl. After drying with $MgSO_4$ and evaporation of the solvent, the residue was subjected to a column chromatography (80% ethyl acetate/hexane) and a mixture of isomers **42** and **43** (1.24 g, 87%) was obtained. This mixture was then separated by preparative TLC (five developments with 50% ethyl acetate/hexane) and the desired pure epimers **42a** and **42b** were obtained in order of elution.

Compound 42a: oil; $[\alpha]_D = +17°$ ($c = 0.80$, $CHCl_3$); ^{1}H NMR ($CDCl_3$): $\delta = 5.95$ (q, $J = 6.8$ Hz, 1H, C*H*Br), 4.96 (d, $J = 9.2$ Hz, 1H, C*H*-CO-Py), 3.93 (m, 1H, C*H*-CH_2OMe), 3.41–3.93 (m, 6H, CH_2OMe + CH_2NCH_2), 3.32 (s, 3H, OCH_3), 2.90 (s, 3H, NCH_3), 1.92 (m, 4H, CH_2CH$_2$NCH$_2$CH_2), 1.82 (d, $J = 6.8$ Hz, CHBrCH_3); ^{13}C NMR ($CDCl_3$): $\delta = 170.3$ (*C*OCHBr), 165.0 (CO), 153.7 (CO), 70.6 (*C*H$_2$OMe), 59.1 (OCH$_3$), 54.8 (*C*H-CO-Py + *C*H-CH$_2$OMe), 46.5 (N*C*H$_2$), 46.2 (N*C*H$_2$), 40.0 (*C*HBr), 29.7 (N*C*H$_3$), 26.2 (NCH$_2$*C*H$_2$), 24.2 (NCH$_2$*C*H$_2$), 21.1 (CH*C*H$_3$).

Compound 42b: white cubes; m.p. 102–103 °C; $[\alpha]_D = -6.8°$ ($c = 0.50$, $CHCl_3$); ^{1}H NMR ($CDCl_3$): $\delta = 5.90$ (q, $J = 6.8$ Hz, 1H, C*H*Br), 4.97 (d, $J = 9.5$ Hz, 1H, C*H*-CO-Py), 3.91 (m, 1H, C*H*-CH$_2$OMe), 3.43–3.89 (m, 6H, CH_2OMe + CH_2NCH_2), 3.31 (s, 3H, OCH_3), 2.91 (s, 3H, NCH_3), 1.95 (m, 4H, CH_2CH$_2$NCH$_2$CH_2), 1.81 (d, $J = 6.8$ Hz, 3H, CHBrCH_3); ^{13}C NMR ($CDCl_3$): $\delta = 169.8$ (*C*OCHBr), 164.2 (CO), 153.7 (CO), 70.7 (*C*H$_2$OMe), 59.1 (O*C*H$_3$), 54.8 (CH), 54.6 (CH), 46.4 (N*C*H$_2$), 46.2 (N*C*H$_2$), 39.2 (*C*HBr), 29.8 (N*C*H$_3$), 26.1 (NCH$_2$*C*H$_2$), 24.2 (NCH$_2$*C*H$_2$), 21.1 (CHBr*C*H$_3$); IR of the epimer mixture **42**: $\tilde{\nu} = 2977$, 2929, 2880, 1733, 1649, 1448, 1649, 1448, 1389, 1245, 1190, 1012 cm^{-1}; MS (FAB+) of the epimer mixture **42**: *m*/*z* (%): 378 (46) $[M+H]^+$, 376 (47) $[M+H]^+$, 231 (62), 155 (27), 154 (100) $[M-HBr-COPy-CH_2OCH_3]^+$, 137 (86), 109 (22); HRMS (FAB+): *m*/*z*: calcd for $C_{14}H_{23}N_3O_4Br$: 376.087193; found: 376.087442.

Compound 43: oil; ^{1}H NMR ($CDCl_3$): $\delta = 5.92$ (m, 1H, C*H*Br), 4.70 (m, 1H, C*H*-CH$_2$OMe), 4.46 (d, $J = 8.4$ Hz, 1H, C*H*-CO-Py of one isomer), 4.39 (d, $J = 8.4$ Hz, 1H, C*H*-CO-Py of one isomer), 3.60 (m, 1H, $^1/_2$ of CH_2OMe), 3.53–3.44 (m, 5H, $^1/_2$ of CH_2OMe + CH_2NCH_2), 3.24 (s, 3H, OCH_3 of one isomer), 3.23 (s, 3H, OCH_3 of one isomer), 2.89 (s, 3H, NCH_3 of one isomer), 2.87 (s, 3H, NCH_3 of one isomer), 1.92 (m, 4H, CH_2CH$_2$NCH$_2$CH_2), 1.82 (d, $J = 6.8$ Hz, CHBrCH_3 of one isomer), 1.79 (d, $J = 6.8$ Hz, CHBrCH_3 of one isomer); ^{13}C NMR ($CDCl_3$): $\delta = 169.7$ (*C*OCHBr of one isomer), 169.5 (*C*OCHBr of one isomer), 164.3 (CO), 153.7 (CO), 67.8 (*C*H$_2$OMe of one isomer), 67.1 (*C*H$_2$OMe of one isomer), 58.8 (OCH$_3$ of one isomer), 58.6 (OCH$_3$ of one isomer), 52.1 (*C*H), 51.3 (*C*H), 46.4 (N*C*H$_2$), 45.8 (N*C*H$_2$), 39.7 (*C*HBr of one isomer), 39.2 (*C*HBr of one isomer), 29.9 (N*C*H$_3$ of one isomer), 29.7 (N*C*H$_3$ of one isomer), 26.1 (NCH$_2$*C*H$_2$), 24.1 (NCH$_2$*C*H$_2$), 21.1 (CHBr*C*H$_3$ of one isomer), 20.5 (CHBr*C*H$_3$ of one isomer); IR: $\tilde{\nu} = 2975$, 2926, 2881, 1736, 1688, 1652, 1447, 1377, 1242, 1189, 1099, 734, 677 cm^{-1}; MS (EI): *m*/*z* (%): 375 (2) $[M]^+$, 295 (10) $[M-HBr]^+$, 279 (99) $[M-COPy]^+$, 277 (100) $[M-COPy]^+$, 143 (83) $[M-COPy-COCH(CH_3)Br]^+$, 111 (22) $[M-COPy-COCH(CH_3)Br-MeOH]^+$, 98 (26) $[COPy]^+$; HRMS (EI+): *m*/*z*: calcd for $C_{14}H_{22}N_3O_4Br$: 375.079368; found: 375.079321.

DKR of 42 by substitution with benzylamine: Benzylamine (16 μL, 0.15 mmol) was added to a stirred solution of both epimers **42** (38 mg, 0.10 mmol), *n*Bu_4NBr or *n*Bu_4NI depending on the experiment (0.2 equiv) and Et_3N (17 μL, 0.12 mmol) in dry THF (1 mL). After 48 h the crude reaction mixture was purified by preparative TLC (10% MeOH/CH_2Cl_2) to yield the substituted product **44**, oil, *de* 99% (*n*Bu_4NBr) and *de* 100% (*n*Bu_4NI) determined by HPLC, *i*PrOH/*n*hexane 20:80, 1.0 mL min^{-1}, $\lambda_{max} = 254$ nm, t_R (**44**) = 13.5, t_R (epimer (*S*)-**44**) = 15.4 min; $[\alpha]_D = +26°$ ($c = 3.0$, $CHCl_3$); ^{1}H NMR ($CDCl_3$): $\delta = 4.97$ (d, $J = 9.6$ Hz, 1H, C*H*-CO-Py), 4.74 (q, $J = 6.8$ Hz, 1H, C*H*(NHCH$_2$Ph)CH$_3$), 3.90 (m, 1H, C*H*-CH$_2$OMe), 3.91–3.44 (m, 8H, CH_2OMe + CH_2NCH_2 + NHCH_2Ph), 3.32 (s, 3H, OCH_3), 2.88 (s, 3H, NCH_3), 1.94 (m, 4H, CH_2CH$_2$NCH$_2$CH_2), 1.34 (d, $J = 6.8$ Hz, 3H, CH(NHCH$_2$Ph)CH_3); ^{13}C NMR ($CDCl_3$): $\delta = 176.9$ (*C*OCH(NHCH$_2$Ph)CH$_3$), 165.1 (CO), 154.1 (CO), 139.6 (*i*Ph), 128.6 (Ph), 128.2 (Ph), 126.8 (Ph), 70.7 (*C*H$_2$OMe), 59.1 (OCH$_3$), 55.0 (*C*H(NHCH$_2$Ph)CH$_3$ + *C*H-CH$_2$OMe), 54.5 (*C*H-CO-Py), 51.4 (CH$_2$Ph), 46.4 (N*C*H$_2$), 46.2 (N*C*H$_2$), 29.7 (N*C*H$_3$), 26.2 (NCH$_2$*C*H$_2$), 24.2 (NCH$_2$*C*H$_2$), 19.1 (CH(NHCH$_2$Ph)*C*H$_3$); IR: $\tilde{\nu} = 3440$, 2963, 2933, 2876, 1733, 1649, 1451, 1390, 1343, 1239, 1105, 749, 701 cm^{-1}; MS (EI): *m*/*z* (%): 403 (1) $[M+H]^+$, 311 (6) $[M-CH_2Ph]^+$, 134 (68), 91 (100) $[PhCH_2]^+$, 56 (20), 55 (25); HRMS (EI+): *m*/*z*: calcd for $C_{21}H_{30}N_4O_4$: 402.226706; found: 402.226782.

Substitution on 42 with benzylamine in the presence of $AgNO_3$: Benzylamine (33 μL, 0.3 mmol) was added to a stirred solution of both isomers **42** (38 mg, 0.1 mmol) and $AgNO_3$ (34 mg, 0.2 mmol) in dry THF (1 mL). After 48 h the crude reaction mixture was purified by preparative TLC (10% MeOH/CH_2Cl_2) to yield the substituted product **44** as mixture of diastereoisomers (39 mg, 97%).

^{1}H NMR (the number of the protons is calculated with respect to the integral of the peak at 4.88 for the minor and at 4.97 for the major product): $\delta = 7.38$–7.20 (m, 5H, Ph), 4.97 (d, $J = 9.6$ Hz, 1H, C*H*-CO-Py^{major} **44**(***R***)), 4.88 (d, $J = 9.7$ Hz, 1H, C*H*-CO-Py^{minor} **44**(*S*)), 4.73–4.79 (m, C*H*(NHCH$_2$Ph)CH$_3$ of both products), 3.39–3.93 (m, C*H*-CH$_2$OMe + CH_2OMe + CH_2NCH_2+ NHCH_2Ph of both products), 3.32 (s, 3H, OCH_3^{major}), 3.31 (s, 3H, OCH_3^{minor}), 2.884 (s, 3H, NCH_3^{major}), 2.876 (s, 3H, NCH_3^{minor}), 1.97 (m, CH_2CH$_2$NCH$_2$CH_2 of both products), 1.37 (d, $J = 6.8$ Hz, 3H, CH(NHCH$_2$Ph)CH_3^{minor}), 1.34 (d, $J = 6.8$ Hz, 3H, CH(NHCH$_2$Ph)CH_3^{major}); ^{13}C NMR ($CDCl_3$): $\delta = 176.9$ (*C*OCH(NHCH$_2$Ph)CH$_3^{major}$), 176.1 (*C*OCH(NHCH$_2$Ph)CH$_3^{minor}$), 165.1 (CO^{major}), 164.8 (CO^{minor}), 154.3 (CO^{minor}), 154.1 (CO^{major}), 139.6 (*i*Ph), 138.9 (*i*Ph), 128.8 (Ph), 128.6 (Ph), 128.2 (Ph), 126.8 (Ph), 70.7 (*C*H$_2$OMe), 59.1 (OCH$_3$), 55.3, 55.0, 54.5, 54.2, 52.0, 51.4, 46.4 (N*C*H$_2$), 46.2 (N*C*H$_2$), 46.0 (N*C*H$_2$), 29.7 (N*C*H$_3^{major}$), 29.6 (N*C*H$_3^{minor}$), 26.2 (NCH$_2$*C*H$_2$), 24.2 (NCH$_2$*C*H$_2$), 19.4 (CH(NHCH$_2$Ph)*C*H$_3^{minor}$), 19.1 (CH(NHCH$_2$Ph)*C*H$_3^{major}$).

Methanolysis of 44: Triethylamine (25 μL, 0.18 mmol) was added to a stirred solution of isomers **44** (58 mg, 0.14 mmol) in methanol (1.5 mL). The reaction was heated under reflux for 24 h. The reaction was allowed to cool to room temperature, the solvent was evaporated and the residue purified by preparative TLC (50% AcOEt/hexane) yielding, as the major enantiomer, (*R*)-methyl 2-(benzylamino)-propionate (**45**; 14 mg, 50%) as a colourless liquid. The spectral data for product **45** are identical to the literature ones.[41] HPLC analysis (*i*PrOH/*n*hexane 5:95, 1.0 mL min^{-1}, $\lambda_{max} = 225$ nm) shows, by comparison with an authentic sample enriched in enantiomer (*R*), $t_R = 6.30$ min (*S* enantiomer, minor product) and $t_R = 6.63$ min (*R* enantiomer, major product).

Acknowledgement

We gratefully acknowledge the Roche Vitamines France for a generous gift of lactone **29**. We gratefully acknowledge the Fundação para a Ciência e a Tecnologia (FCT) and FEDER (Ref. POCTI/QUI/42983/2001) for financial support and a grant to A.G.S. (Ref. BSAB/159/00). We gratefully acknowledge the Calouste Gulbenkian Foundation for support.

[1] I. Suzuki, H. Kin, Y. Yamamoto, *J. Am. Chem. Soc.* **1993**, *115*, 10139–10146.
[2] P. N. Devine, U.-H. Dolling, R. M. Heid, D. M. Tschaen, *Tetrahedron Lett.* **1996**, *37*, 2683–2686.
[3] J. A. O′Meara, N. Gardee, M. Jung, R. N. Ben, T. Durst, *J. Org. Chem.* **1998**, *63*, 3117–3119.
[4] P. Camps, F. Pérez, N. Soldevilla, *Tetrahedron: Asymmetry* **1997**, *8*, 1877–1894.
[5] P. Camps, F. Pérez, N. Soldevilla, M. A. Borrego, *Tetrahedron: Asymmetry* **1999**, *10*, 493–509.
[6] R. S. Ward, A. Pelter. D. Goubet, M. C. Pritchard, *Tetrahedron: Asymmetry* **1995**, *6*, 93–96.

[7] R. S. Ward, A. Pelter. D. Goubet, M. C. Pritchard, *Tetrahedron: Asymmetry* **1995**, *6*, 469–498.
[8] S. Hanessian, Y. L. Bennani, *Tetrahedron Lett.* **1990**, *31*, 6465–6468.
[9] V. J. Blazis, K. J. Koeller, C. D. Spilling, *J. Org. Chem.* **1995**, *60*, 931–937.
[10] H. Roder, G. Helmchen, E.-M. Peters, K. Peters, H.-G. Schnering, *Angew. Chem.* **1984**, *96*, 895–896; *Angew. Chem. Int. Ed. Engl.* **1984**, *23*, 898–899.
[11] D. A. Evans, J. Bartroli, T. L. Shih, *J. Am. Chem. Soc.* **1981**, *103*, 2127–2129.
[12] D. A. Evans, M. D. Ennis, D. J. Mathre, *J. Am. Chem. Soc.* **1982**, *104*, 1737–1739.
[13] D. A. Evans, *Aldrichimica Acta* **1982**, *15*, 23–32.
[14] D. A. Evans, M. M. Morrissey, R. L. Dorow, *J. Am. Chem. Soc.* **1985**, *107*, 4346–4348.
[15] I. Abrahams, M. Motevalli, A. J. Robinson. P. B. Wyatt, *Tetrahedron* **1994**, *50*, 12755–12772.
[16] A. Abdel-Magid, L. N. Pridgen, D. S. Eggleston, I. Lantos, *J. Am. Chem. Soc.* **1986**, *108*, 4595–4602.
[17] D. A. Evans, A. E. Weber, *J. Am. Chem. Soc.* **1986**, *108*, 6757–6761.
[18] D. A. Evans, K. T. Chapman, J. Bisaba, *J. Am. Chem. Soc.* **1988**, *110*, 1238–1256.
[19] A. G. Santos, S. X. Candeias, C. A. M. Afonso, K. Jenkins, S. Caddick, N. R. Treweeke, D. Pardoe, *Tetrahedron* **2001**, *57*, 6607–6614.
[20] G. Cardillo, L. Gentilucci, M. Gianotti, A. Tolomelli, *Org. Lett.* **2001**, *3*, 1165–1167.
[21] E. Nicolás, K. C. Russel, J. Knollenberg, V. J. Hruby, *J. Org. Chem.* **1993**, *58*, 7565–7571.
[22] G. Li, M. A. Jarosinski, V. J. Hruby, *Tetrahedron Lett.* **1993**, *34*, 2561–2564.
[23] K. J. Hale, J. Cai. V. Delisser, S. Manaviazar, S. A. Peak, G. S. Bhatia, T. C. Collins, N. Jogiya, *Tetrahedron* **1996**, *52*, 1047–1068.
[24] J. H. Wu, R. Radinov, N. A. Porter, *J. Am. Chem. Soc.* **1995**, *117*, 11029–11030.
[25] M. P. Sibi, J. Ji, *J. Org. Chem.* **1996**, *61*, 6090–6091.
[26] M. P. Sibi, C. P. Jasperse, J. Ji, *J. Am. Chem. Soc.* **1995**, *117*, 10779–10780.
[27] M. P. Sibi, J. Ji, *J. Am. Chem. Soc.* **1996**, *118*, 9200–9201.
[28] Y. Yamamoto, S. Onuki, M. Yumoto, N. Asao, *J. Am. Chem. Soc.* **1994**, *116*, 421–422.
[29] C. L. Mero, N. A. Porter, *J. Am. Chem. Soc.* **1999**, *121*, 5155–5160.
[30] For reviews in DKR, see: a) U. T. Strauss, U. Felfer, K. Faber, *Tetrahedron: Asymmetry* **1999**, *10*, 107–117; b) S. Caddick, K. Jenkins, *Chem. Soc. Rev.* **1996**, *25*, 447–456; c) R. S. Ward, *Tetrahedron: Asymmetry* **1995**, *6*, 1475–1490; d) R. Noyori, M. Tokunaga, M. Kitamura, *Bull. Chem. Soc. Jpn.* **1995**, *68*, 36–56.
[31] S. Caddick, S. Jenkins, *Tetrahedron Lett.* **1996**, *37*, 1301–1304.
[32] S. Caddick, S. Jenkins, N. Treweeke, S. X. Candeias, C. A. Afonso, *Tetrahedron Lett.* **1998**, *39*, 2203–2206.
[33] J. A. O'Meara, M. Jung, T. Durst, *Tetrahedron Lett.* **1995**, *36*, 2559–2562.
[34] H. Kubota, A. Kubo, K. Nunami, *Tetrahedron Lett.* **1994**, *35*, 3107–3110.
[35] K. Nunami, H. Kubota, A. Kubo, *Tetrahedron Lett.* **1994**, *35*, 8639–8642.
[36] H. Kubota, A. Kubo, M. Takahashi, R. Shimizu, T. Da-te, K. Okamura, K. Nunami, *J. Org. Chem.* **1995**, *60*, 6776–6784.
[37] A. Kubo, M. Takahashi, H. Kubota, K. Nunami, *Tetrahedron Lett.* **1995**, *36*, 6251–6252.
[38] A. Kubo, H. Kubota, M. Takahashi, K. Nunami, K. *Tetrahedron Lett.* **1996**, *37*, 4957–4960.
[39] A. Kubo, H. Kubota, M. Takahashi, K. Nunami, *J. Org. Chem.* **1997**, *62*, 5830–5837.
[40] J. Clariana, N. Gálvez, C. Marchi, M. Moreno-Mañas, A. Vallribera, E. Molins, *Tetrahedron* **1999**, *55*, 7331–7344.
[41] S. Caddick, C. A. M. Afonso, S. X. Candeias, P. B. Hitchcock, K. Jenkins, L. Murtagh, D. Pardoe, A. G. Santos, N. R. Treweeke, R. Weaving, *Tetrahedron* **2001**, *57*, 6589–6605.
[42] Spartan '02, Wavefunction, Inc. Irvine, CA.
[43] Gaussian 98, Revision A.7, M. J. Frisch, G. W. Trucks, H. B. Schlegel, G. E. Scuseria, M. A. Robb, J. R. Cheeseman, V. G. Zakrzewski, J. A. Montgomery, Jr., R. E. Stratmann, J. C. Burant, S. Dapprich, J. M. Millam, A. D. Daniels, K. N. Kudin, M. C. Strain, O. Farkas, J. Tomasi, V. Barone, M. Cossi, R. Cammi, B. Mennucci, C. Pomelli, C. Adamo, S. Clifford, J. Ochterski, G. A. Petersson, P. Y. Ayala, Q. Cui, K. Morokuma, D. K. Malick, A. D. Rabuck, K. Raghavachari, J. B. Foresman, J. Cioslowski, J. V. Ortiz, A. G. Baboul, B. B. Stefanov, G. Liu, A. Liashenko, P. Piskorz, I. Komaromi, R. Gomperts, R. L. Martin, D. J. Fox, T. Keith, M. A. Al-Laham, C. Y. Peng, A. Nanayakkara, C. Gonzalez, M. Challacombe, P. M. W. Gill, B. Johnson, W. Chen, M. W. Wong, J. L. Andres, C. Gonzalez, M. Head-Gordon, E. S. Replogle, J. A. Pople, Gaussian, Inc., Pittsburgh PA, **1998**.
[44] S. Tsuzuki, H. P. J. Lüthi, *Chem. Phys.* **2001**, *114*, 3949–3957.
[45] F. Moreau, D. Florentin, A. Marquet, *Tetrahedron* **2000**, *56*, 285–293.
[46] S. X. Candeias, K. Jenkins, C. A. M. Afonso, S. Caddick, *Synth. Commun.* **2001**, *31*, 3241–3254.
[47] N. Finch, J. J. Fitt, I. H. S. Hsu, *J. Org. Chem.* **1975**, *40*, 206–215.
[48] K. Hayashi, K. Nunami, J. Kato, N. Yoneda, M. Kubo, T. Ochiai, R. Ishida, *J. Med. Chem.* **1989**, *32*, 289–297.

Received: May 24, 2004
Published online: November 18, 2004

